

A STUDY OF THE HUMAN VISUAL EVOKED POTENTIAL

by

JOHN REAVELY BENNETT

B.Sc., Queen's University, 1966

A THESIS SUBMITTED IN PARTIAL FULFILMENT OF THE
REQUIREMENTS FOR THE DEGREE OF

MASTER OF APPLIED SCIENCE

in the Department of
Electrical Engineering

We accept this thesis as conforming to the
required standard

Research Supervisor

Members of Committee

Head of Department.

Members of the Department
of Electrical Engineering

THE UNIVERSITY OF BRITISH COLUMBIA

December, 1968

In presenting this thesis in partial fulfilment of the requirements for an advanced degree at the University of British Columbia, I agree that the Library shall make it freely available for reference and Study.

I further agree that permission for extensive copying of this thesis for scholarly purposes may be granted by the Head of my Department or by his representatives. It is understood that copying or publication of this thesis for financial gain shall not be allowed without my written permission.

Department of ELECT. ENG.

The University of British Columbia
Vancouver 8, Canada

Date DEC. 20/68

ABSTRACT

A new approach to the study of the human Visual Evoked Potential is described, based on a simple model of the visual system. This model is then used as a tool for the investigation of the visual system and its characteristics. Certain assumptions are made concerning the spontaneous brain activity accompanying the visual response and this activity is then described by its probability density and auto-correlation functions. A theoretical basis is described for the two noise reduction techniques of ensemble averaging and the sliding mean and the implications of these processing procedures as applied to the visual system are discussed with reference to the system model. The theoretical assumptions of this analysis are then experimentally investigated. The nature of the visual response is discussed and it is shown that this response can be subdivided into two components on the basis of their time behaviour. Each of these two components, the V.E.P. and the Rhythmic After-discharge is investigated in detail. The relation of the Alpha Rhythm to the After-discharge is also investigated using auto-correlation techniques. Finally, a statistical model for the V.E.P. is described as a means for studying and applying the visual response, its uses being discussed in some detail.

An electronic coding scheme was designed to facilitate the cataloguing of experimental data, and is described in the Appendix.

TABLE OF CONTENTS

	Page
LIST OF ILLUSTRATIONS.....	iv
LIST OF TABLES.....	vi
ACKNOWLEDGEMENT.....	vii
1. INTRODUCTION.....	1
2. THE VISUAL EVOKED POTENTIAL AND THE VISUAL SYSTEM.....	4
2.1 The System Model.....	4
2.2 The Mathematical Model for the Averaging Process...	8
2.3 The Mathematical Model for the Application of the Sliding Mean.....	11
2.4 Correlation on a Digital Computer.....	17
2.5 The V.E.P. Detection and Processing.....	21
2.6 Experimental Verification of the Theoretical Assumptions of the Model of the Visual System.....	26
3. THE ENVIRONMENT.....	31
3.1 Physical Environment.....	31
3.2 Linearity and Time Behaviour of the Visual System..	41
3.3 The Nature of the Visual Response.....	48
4. A STATISTICAL MODEL FOR THE V.E.P.....	55
4.1 The Distribution of the Data.....	55
APPENDIX I - Technical Specifications.....	67
APPENDIX II - The Logic Interface.....	68
APPENDIX III - Data Cataloguing System.....	72
REFERENCES.....	78

LIST OF ILLUSTRATIONS

Figure		Page
2.1.1	The Main Components of the Visual System.....	5
2.1.2	The Model of the Visual System.....	6
2.3.1	The Noise Reduction Process.....	16
2.4.1	Normalized Auto-Correlogram Estimates.....	20
2.5.1	Data Processing.....	25
2.6.1	The "Goodness of Fit" of the Noise Data to the Gaussian Distribution.....	29
2.6.2	Normalized Noise Auto-Correlogram Estimates.....	30
3.1.1	The Human Brain Showing the Relationship Between Electrode Position and the Visual Cortex.....	33
3.1.2	Electrode Placement Showing the Mounting Appara- tus with the Electrode Cross and Amplifier Leads in Place.....	35
3.1.3	Monopolar vs Bipolar Responses.....	37
3.1.4	The Human Eye Showing the Main Components and Angles Subtended by the Macula and the Fovea.....	39
3.2.1	The Relation of Stimulus Size to V.E.P. Pattern...	42
3.2.2	The Relation of Stimulus Intensity to V.E.P. Pattern.....	44
3.2.3	The Individual Consistency in Three Subjects Over Ten Months.....	47
3.3.1	Mean Visual Evoked Potentials.....	50
3.3.2	Sample Visual Responses.....	52
4.1.1	Goodness of Fit of the Latency of Electrode Number One to the Gaussian Distribution.....	59
4.1.2	Goodness of Fit of the Amplitude of Electrode Number One to the Gaussian Distribution.....	59
4.1.3	Acceptability Scheme for Electrode Number One.....	62
4.1.4	Acceptability Scheme for Electrode Number Two.....	62
4.1.5	Acceptability Scheme for Electrode Number Three...	63

4.1.6	Acceptability Scheme for Electrode Number Four.....	63
A2-1	Data Transfer Sequence.....	69
A2-2	Paper Punch Interface.....	71
A3-1	Digital Encoder.....	74
A3-2	Digital Decoder.....	77

LIST OF TABLES

		Page
Table 3.3.1A	Mean Values of Latency and Amplitude as Computed by Ciganěk.....	51
Table 3.3.1B	Mean Values of Latency and Amplitude as Computed by Bennett.....	51
Table 3.3.2	Comparison of E.E.G. Frequencies with those of the After-discharge.....	54
Table 4.1.1	Comparison of the Latency and Amplitude of the Major Deflections of the Four Electrode Positions.....	56
Table 4.1.2	Chi-Square "Goodness of Fit" Test Results for the Fitting of the V.E.P. Data to the Gaussian Distribution.....	58

ACKNOWLEDGEMENT

Acknowledgement is most gratefully given to the National Research Council for their financial support through the studentship and to the Medical Research Council, grant number 67-7264, for their financial support of the research.

I would also like to express my sincerest thanks to Dr. J. S. MacDonald for his guidance and recommendations during the project, to Dr. R. W. Donaldson for his reading and constructive criticism of the thesis and to Dr. K. Uenoyama for his invaluable guidance and assistance in the experimental work.

Finally, I would like to thank Mr. A. Leugner for his help in the construction of the circuit hardware, to my fellow students who proofread the thesis, and to Avis Hopkins for typing the manuscript.

1. INTRODUCTION

When the human eye is stimulated with a pulse of light energy, electrical potential variations are evoked and can be detected at the surface of the scalp over the region of the visual cortex. These potential variations constitute what is known as the Visual Evoked Potential and have been the subject of much interest and controversy in recent years. Of particular interest is the possible use of the Visual Evoked Potential as a clinical diagnostic tool, specifically, as a means of detecting abnormalities in a particular visual system. Fundamental to this type of application are; first, the consistency in time of some characteristic of the Visual Evoked Potential obtained from any normal individual, and second, the presence of that characteristic in at least part if not all of the general population.

In most published work to date concerning the Visual Evoked Potential, it has been assumed that, within reasonable limits, a consistent response can be obtained from any one individual over prolonged periods of time. This assumption has been experimentally investigated^(1,2). Both authors have demonstrated that the degree of consistency in the general pattern of the response varies from individual to individual and that large variations in amplitude can be expected over time periods of a few days.

Concerning the subject of inter-individual similarities in the Visual Evoked Potential, very little consistency has been reported, and, in fact, it has been suggested⁽¹⁾, that this response may someday be used as a measure of individuality. Notable exceptions to this however, have been reported by Ciganék⁽³⁾ and Creutzfeldt and Kuhnt⁽⁴⁾.

Ciganék has proposed a model for the Visual Evoked Potential based on the distribution of seven major potential deflections observed in the first 250 msec of the response, and reports good consistency over a population sample of forty-five subjects.

Creutzfeldt and Kuhnt also claim good consistency in thirty subjects and have proposed a model based on the ensemble average of the thirty individual ensemble averages. Their model differs from that of Ciganék both in the number and latency of deflections observed.

This thesis represents an investigation into the exact nature of the Visual Evoked Potential and its possible application in clinical diagnostics. As an aid to this investigation, a simple communication system is proposed as a model of the visual system. While some consideration was given to the physiological processes involved, the model was proposed primarily on the basis of the input-output relationships observed in experimentation and is not intended as an accurate representation of the internal visual processes. It does, however, serve as a useful tool for the analysis of these processes.

The experimental results used in this thesis are based on responses obtained from sixty patients in all, six of whom were studied on several occasions over a period of ten months. The subjects were male, between the ages of 20 and 80 years, predominantly 50 to 75. The stimulus in all experiments consisted of a pulse of white light applied to the central foveal area of the retina. Special data processing equipment included a computer of average transients interfaced to a PDP-9 digital data processing computer, combining the advantages of on-line monitoring of the data as it was accumulated with speed and flexibility of data processing and analysis off-line.

A first study was done to determine the extent of the individual consistency over the ten month period in order to clarify the

seeming discrepancies in the literature and to classify the proposed model with respect to time variance or invariance. The linearity of the system was also investigated with respect to stimulus size and intensity, and the results compared with those of Vaughan⁽⁵⁾. The relationship between the Visual Evoked Potential and the intrinsic Alpha Rhythm is discussed with reference to pertinent literature and experimental results.

A model for the Visual Evoked Potential is proposed and compared with those of Ciganěk and Creutzfeldt and Kuhnt. It is shown that the parameters of the model are Gaussian distributed and 95% statistical limits are determined for the normal response. An algorithm is outlined to identify the normality or abnormality of a given Visual Evoked Potential on the basis of the model.

2. THE VISUAL EVOKED POTENTIAL AND THE VISUAL SYSTEM

2.1 The System Model

For the purposes of this thesis, the Visual Evoked Potential (V.E.P.) is defined as the totality of the potential variations observed at the surface of the human scalp which are synchronized with a light stimulus applied to either or both retinas of the eyes.

The V.E.P. as defined is submerged in further potential variations reflecting spontaneous brain activity resulting from other bodily functions and mental processes. Since this spontaneous activity is unsynchronized with the stimulus, it can be regarded as "noise" and the actual evoked potential as the "signal". The "signal" to "noise" ratio is about 1/25 for an average system.

The visual system referred to in this thesis is defined as the totality of all components of the nervous system which influence the pattern of the V.E.P. in the absence of the spontaneous brain "noise". The main components of the visual system are shown in Fig. 2.1.1. While a detailed description of the physiology of the visual system is outside the scope of this thesis, a general description of the signal flow through the system is included. For more detailed information on this subject, the reader is referred to Wolf⁽⁷⁾.

At the input stage, the light pulse is focused on the posterior hemisphere of the eye where it is converted to electrical pulses by an elaborate arrangement of specialized nerve cells located within the retina. The topography of the retina is described in further detail in Section 3.2. The outputs of these "transducers" are fed into a complex processing network of nerve cells which terminate in the visual fibres of the optic nerve. The signal information is then transmitted along the fibres of the optic nerve to the

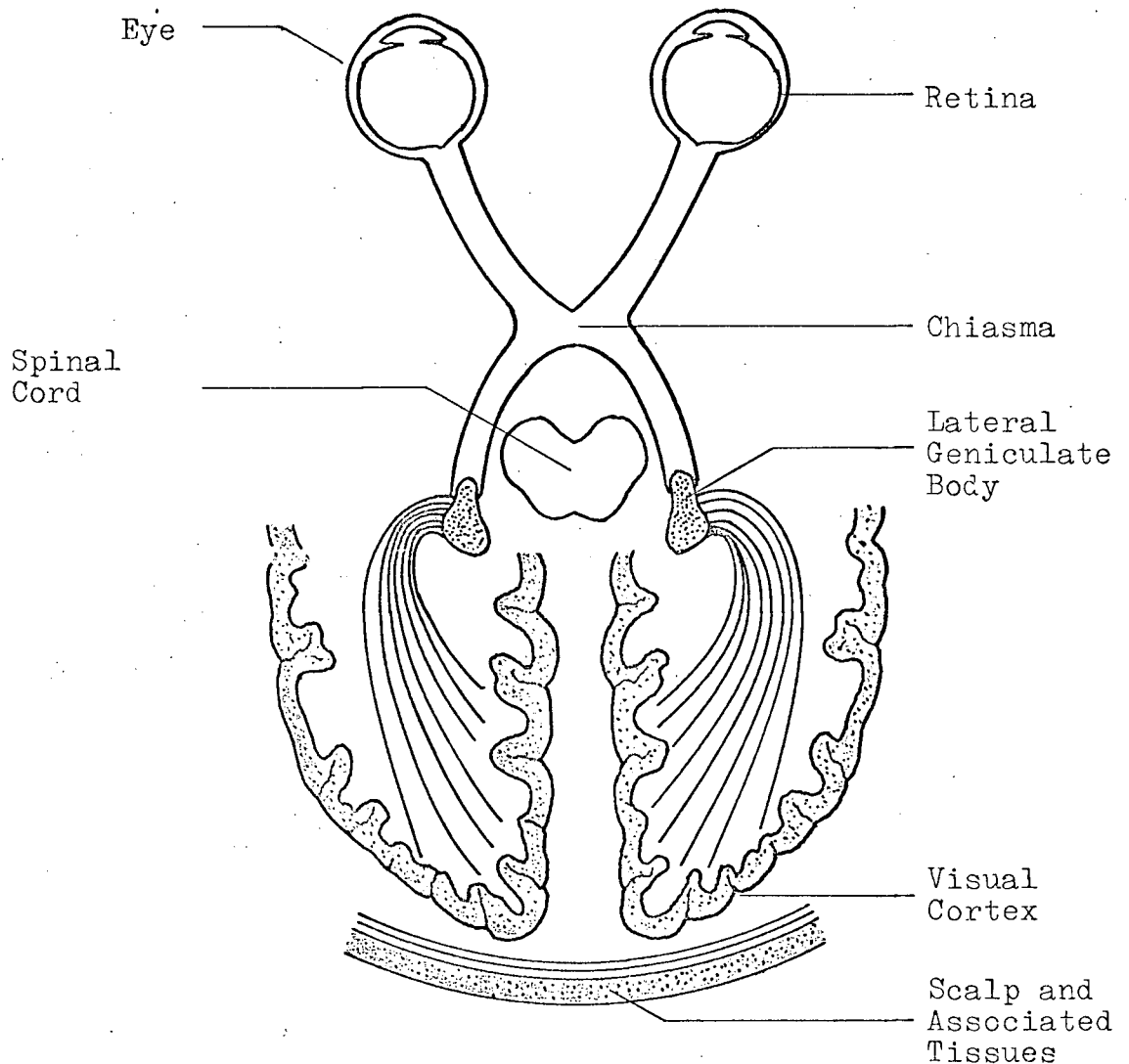


Fig. 2.1.1 The Main Components of the Visual System

chiasma. Within the chiasma, the signals from the two eyes cross, with most of the information from the right eye proceeding on to the left lateral geniculate body and that from the left eye proceeding on to the right lateral geniculate body. From the lateral geniculate bodies, the information enters the two sides of the visual cortex where further processing and distribution to other parts of the brain occurs.

The potential patterns observable at the surface of the brain, while they are not the actual information carriers, are an accurate "reflection" of the totality of neural responses within the immediate cortical regions.* Hence, these patterns will reflect not only the information from the visual process, but also information from other parts of the central and peripheral nervous systems. This additional information constitutes what has been previously referred to as noise.

From the brain surface, the potential patterns pass through the skull and associated tissues to the scalp surface where they are detected by the electrodes.

A simplified block diagram of a model of the visual system is illustrated in Fig. 2.1.2. In this model, $v(t)$ represents the transfer characteristics of the retinas, the chiasma, the lateral geniculate

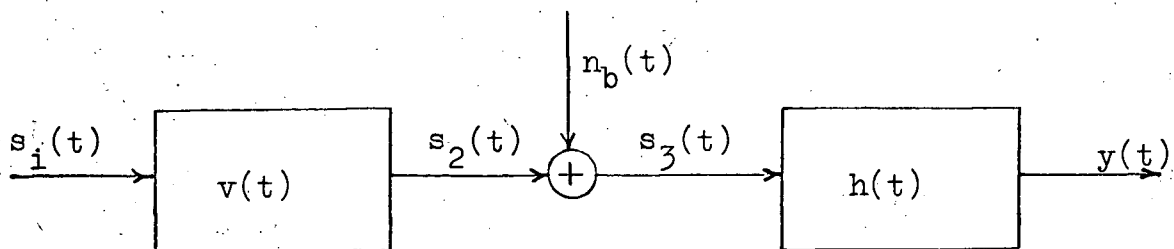


Fig. 2.1.2 The Model of the Visual System for a Fixed Input.

*Sances and Larson⁽⁸⁾ have shown that in fact, the V.E.P. originates within 2 mm of the brain surface.

** Assuming fixed input conditions.

bodies, and all portions of the brain concerned with the visual process in such a way as to influence the pattern of the V.E.P. At this point, no assumptions are made concerning the nature of $v(t)$ although its linearity and time behaviour are investigated in Chapter 3. The output of $v(t)$, the signal $s_2(t)$, represents the portion of the "reflected" potential patterns at the brain surface due to the responses of the neurons of the visual cortex. It will be shown in later sections, that the noise $n_p(t)$ can be approximated by a zero-mean, stationary, Gaussian process, statistically independent of the signal $s_2(t)$. While the results and methods of this thesis do not depend on these assumptions, it will be seen that certain simplifications result in the mathematical analysis of the noise reduction processes if these assumptions can be made.

The transfer function of the skull and associated tissue layers is represented by $h(t)$, and is assumed to be both linear and time-invariant, partly on the basis of physiological considerations*, and partly on the work of Sances and Larson⁽⁸⁾ who have found that the V.E.P. is similar in pattern to the patterns observed near the surface of the brain.

While these assumptions are not mandatory to the study of the V.E.P., they do affect its usefulness as a diagnostic tool. If $h(t)$ is linear and time-invariant, the V.E.P. is a more workable representation of the potential variations at the surface of the brain and hence of the activity of the visual system. That is, all non-

* While the transfer function of the skull and associated tissues has not been fully investigated experimentally, it is not likely that significant changes would occur in its frequency response or attenuation characteristics either in time or with signal variations. For these reasons, linearity and time-invariance are assumed.

linearities and time-variance can then be attributed to the visual process itself, and not to the combination of two phenomena, one of which has no relation to the visual process at all.

A second advantage of the previous assumptions is as follows. If $n_b(t)$ is stationary, zero-mean, Gaussian and statistically independent of $s_2(t)$, the output noise $n(t)$ will also be statistically independent of the output signal $s(t)$ or the V.E.P., and stationary, zero-mean and Gaussian as well. Mathematically,

$$y(t) = s(t) + n(t)$$

$$y(t) = \int_{-\infty}^{+\infty} s_2(\tau)h(t-\tau)d\tau + \int_{-\infty}^{+\infty} n(\tau)h(t-\tau)d\tau. \quad 2.1$$

Finally, these assumptions are also simplifying in the application of two noise reduction techniques to be outlined in the following sections. In these sections, it is shown that by the application of these techniques, the output noise $n(t)$ can be reduced to a negligible minimum and hence the second term in Equation 2.1 is effectively zero. The remaining signal, the V.E.P., is simply a linear transformation of the activity at the surface of the brain and hence of the visual system.

2.2 The Mathematical Model for the Averaging Process

It has been previously assumed that the output of the visual system can be subdivided into the sum of two statistically independent components: a signal $s(t)$ which can be assumed at this stage to have a mean ensemble value $\langle s(t) \rangle$, and an ensemble variance $\sigma_s^2(t)$; and a noise component, $n(t)$, which is stationary, zero-mean, and Gaussian with variance $\sigma_n^2(t)$. The equations governing the output of such a system are simply;

$$y(t) = s(t) + n(t)$$

$$\langle y(t) \rangle = \langle s(t) \rangle + \langle n(t) \rangle$$

$$\sigma_y^2(t) = \sigma_s^2(t) + \sigma_n^2(t).$$

where the triangular brackets represent the sample mean value and $\sigma_y^2(t)$ represents the variance of $y(t)$.

In addition to the assumptions already made concerning the system and its output, one further assumption is useful in the application of the ensemble averaging technique; namely, that two samples of the noise separated in time by the sample time interval, be uncorrelated. In Chapter 3, this assumption is experimentally investigated and shown to be approximately true.

The ensemble averaging technique consists of stimulating the system N times, and algebraically adding the N outputs in such a way that corresponding sample instants which are time-locked to the stimulus, are added together. The result is then divided by N . Hence the sample mean of the output at any instant in time (t_i) will be given by the equation:

$$\langle y(t_i) \rangle = \frac{1}{N} \sum_{k=1}^N (s_k(t_i) + n_k(t_i))$$

$$= Z(t_i).$$

In the averaging process, the signal is digitized into a finite number (p) of discrete values, each one corresponding to the amplitude of the signal at some fixed time t_i . Hence the output of this process can be described as a p dimensional "vector" on a time-magnitude plane. In vector notation then, the output of the process can be written:

$$\vec{Z}(t) = \begin{bmatrix} Z(t_1) \\ \vdots \\ Z(t_i) \\ \vdots \\ Z(t_p) \end{bmatrix} .$$

In the limit, as $N \rightarrow \infty$;

$$Z(t_i)_{N=\infty} = E \{s(t_i)\} + E \{n(t_i)\}$$

and since we have assumed the noise to have zero mean;

$$Z(t_i)_{N=\infty} = E \{s(t_i)\} .$$

Hence, in the theoretical limit of an infinite number of samples in the average, the noise could be totally eliminated from the output leaving the undistorted V.E.P. In practical experimentation however, it was found that a reasonable value for N was about 128 and as a result, the noise was not totally eliminated. Nevertheless, the averaging process when used with a finite N , improves the signal-to-noise ratio by decreasing the noise variance.

The theory of noise reduction by ensemble averaging is well known and will not be repeated in this thesis in detail. For a complete theoretical development of the mathematical relationships stated in this section, the reader is referred to Bendat⁽⁹⁾. In the theory of ensemble averaging, it is shown that the variance of the averaged signal is reduced by $1/N$, where N again is the number of signals averaged. For the system under consideration, the variance relationships are:

$$\begin{aligned} \sigma_z^2(t_i) &= \frac{1}{N} \sigma_y^2(t_i) \\ &= \frac{1}{N} \left[\sigma_s^2(t_i) + \sigma_n^2(t_i) \right] . \end{aligned}$$

If $\sigma_s^2(t_i) = 0$, that is, if the signal variance is zero, or alternatively, if the system is time-invariant,* then the variance of the output can be attributed entirely to the noise $n(t)$; and the square root of the variance, the standard deviation, can be used as a reasonable figure for assessing improvement in the signal to noise ratio. Hence an improvement in the signal-to-noise ratio of a factor of \sqrt{N} can be expected.

The signal-to-noise ratio of the visual response was found to vary considerably among subjects and from day to day with any one individual. While in some cases the ensemble averaging technique proved sufficient to reduce the noise to acceptable levels, such was not the case on many occasions and further noise reduction procedures were necessary. Since increasing the number of samples in the ensemble average was not a practical solution for reasons of time and subject discomfort, a second noise reduction technique, the sliding mean, was chosen and is discussed in the following section.

2.3 The Mathematical Model for the Application of the Sliding Mean

In addition to on-line ensemble averaging, a second technique, the sliding mean was used off-line to further reduce the noise level in the signal. The application of this technique was facilitated in two ways. First, since in the data processing procedure, the output of the ensemble averaging process was digitized and stored on paper tape compatible with the PDP-9 data processing computer, the sliding mean could be performed quickly and efficiently. Secondly, the assumptions pertinent to the theory of the sliding mean, i.e., statistically independent, zero-mean, Gaussian and uncorrelated noise

* The validity of this assumption is also investigated in Chapter 3.

have all been previously investigated for the ensemble averaging process.*

It has been shown that the output of the ensemble averaging process can be written in vector form as:

$$\vec{z}(t) = \begin{bmatrix} z(t_1) \\ \vdots \\ z(t_i) \\ \vdots \\ z(t_p) \end{bmatrix},$$

where $z(t_i)$ represents the ensemble average at time t_i , and P , the number of such discrete averages taken of the signal.

If the sampling rate of the averaging process is n samples per second, the length of the signal examined will be P/n seconds.

The output of the sliding mean process is a vector of, in general $P-L$ dimensions, where L can assume a value between 1 and $P-1$. The i th component of the sliding mean vector is given by the equation

$$m(t_i) = \frac{1}{L} \sum_{j=i}^{i+L} z(t_j)$$

The sliding mean output is then described by the vector

$$\vec{M}(t) = \begin{bmatrix} m(t_1) \\ \vdots \\ m(t_i) \\ \vdots \\ m(t_{p-L}) \end{bmatrix}.$$

Applying this technique to the output of the system model,

* Actually, the sliding mean theory assumes that adjacent samples of noise are uncorrelated rather than samples separated by 1 second as in the ensemble averaging process. The assumption of adjacent uncorrelated noise samples is a much more stringent assumption and is only approximated in the physical world. (see Section 2.6) Hence, the theoretical results can only be regarded as valid to the extent of this approximation.

$$m(t_i) = \frac{1}{L} \sum_{j=i}^{i+L} (s_z(t_j) + n_z(t_j))$$

where

$$s_z(t_j) = \frac{1}{N} \sum_{k=1}^N s_k(t_i)$$

and

$$n_z(t_j) = \frac{1}{N} \sum_{k=1}^N n_k(t_i)$$

as in the previous section.

Since $n(t)$ is essentially a continuous process to which the V.E.P. has been added, the samples of noise can be assumed to form an ergodic process and therefore the time and ensemble averages of both $n_k(t_i)$ and $n_z(t_i)$ will be equal.* Consequently, if L is sufficiently large, the average over L adjacent samples will be approximately zero. The previous equation can therefore be rewritten as

$$m(t_i) = \left\langle s_z(t_i) \right\rangle_{T,L} \quad L \rightarrow \infty .$$

It can be seen from this equation, that an irreversible transformation has been performed on the signal $z(t_i)$, but at this expense, the noise has been theoretically eliminated. In actual practice, the choice of L is made on the basis of a compromise between effective noise elimination and desired signal alteration according to this transformation equation. However, the effect of a finite L is to reduce the noise variance, as will be shown.

The variance of the sliding mean output can be expressed as

$$\sigma_m^2(t_i) = \left\langle m(t_i)^2 \right\rangle_{T,L} - \left\langle m(t_i) \right\rangle_{T,L}^2 \quad 2.3.1$$

where $\left\langle m(t_i) \right\rangle_{T,L}$ corresponds to the expected value of $m(t_i)$ for L points in the time average.

* Stationarity, which has been assumed in this statement, is discussed in Section 2.6.

This expected value is the theoretical mean of an infinite number of samples of $m(t_i)$. We define $z(t_{ik})$ as a single sample value at time t_k , and hence

$$m(t_i) = \frac{1}{L} \sum_{k=i}^{i+L} z(t_{ik}).$$

Analysing each term of equation 2.3.1 in turn and substituting for $m(t_i)$:

$$\begin{aligned} \langle m(t_i)^2 \rangle_{T,L} &= \left\langle \frac{1}{L^2} \sum_{k=i}^{i+L} \sum_{j=i}^{i+L} z(t_{ik}) z(t_{ij}) \right\rangle_{T,L} \\ &= \frac{1}{L^2} \sum_{k=i}^{i+L} \sum_{j=i}^{i+L} \left\langle \left\{ s_z(t_{ik}) + n_z(t_{ik}) \right\} \left\{ s_z(t_{ij}) \right. \right. \\ &\quad \left. \left. + n_z(t_{ij}) \right\} \right\rangle_{T,L} \\ &= \frac{1}{L^2} \sum_{k=i}^{i+L} \sum_{j=i}^{i+L} \left\langle s_z(t_{ik}) s_z(t_{ij}) + n_z(t_{ik}) s_z(t_{ij}) \right. \\ &\quad \left. + n_z(t_{ij}) s_z(t_{ik}) + n_z(t_{ik}) n_z(t_{ij}) \right\rangle_{T,L} \end{aligned}$$

2.3.2

We have assumed that adjacent noise samples are uncorrelated.

Therefore,

$$\langle n_z(t_{ik}) n_z(t_{ij}) \rangle_{T,L} = 0 \quad k \neq j$$

Also, since the noise is zero-mean, and $s_z(t_i) + n_z(t_i)$ are independent,

$$\left\langle n_z(t_{ik})s_z(t_{ij}) \right\rangle_{T,L} = \left\langle n_z(t_{ik})s_z(t_{ij}) \right\rangle_{T,L} = 0 .$$

Finally, in Chapter 3, it is shown that the V.E.P. can be regarded as a time-invariant process for any one system. Therefore, the signal $s_z(t_{ik})$ is a constant. Equation 2.3.2 can therefore be rewritten in the form;

$$\left\langle m(t_i)^2 \right\rangle_{T,L} = \frac{1}{L^2} \sum_{k=i}^{i+L} \left\langle s_z(t_{ik}) \right\rangle_{T,L}^2 + \frac{1}{L^2} \sum_{k=i}^{i+L} \left\langle n_z^2(t_{ik}) \right\rangle_{T,L} .$$

Similarly we can write

$$\left\langle m(t_i) \right\rangle_{T,L}^2 = \frac{1}{L^2} \sum_{k=i}^{i+L} \left\langle s_z(t_{ik}) \right\rangle_{T,L}^2 .$$

Therefore,

$$\begin{aligned} \sigma_m^2(t_i) &= \frac{1}{L^2} \sum_{k=i}^{i+L} \left\{ \left\langle s_z(t_{ik}) \right\rangle_{T,L}^2 - \left\langle s_z(t_{ik}) \right\rangle_{T,L}^2 \right\} \\ &\quad + \frac{1}{L^2} \sum_{k=i}^{i+L} \left\langle n_z^2(t_{ik}) \right\rangle_{T,L} . \end{aligned}$$

Since it has been assumed that the signal $s_z(t_{ik})$ is a constant and therefore has zero variance,

$$\sigma_m^2(t_i) = \frac{1}{L^2} \sum_{k=i}^{i+L} \left\langle n_z^2(t_{ik}) \right\rangle_{T,L}$$

$$\sigma_m^2(t_i) = \frac{1}{L} \left\langle n_z^2(t_i) \right\rangle_{T,L} .$$

Again, since the noise process is ergodic,

$$\left\langle n_z^2(t_i) \right\rangle_{T,L} = E \left\{ n_z^2(t_i) \right\}$$

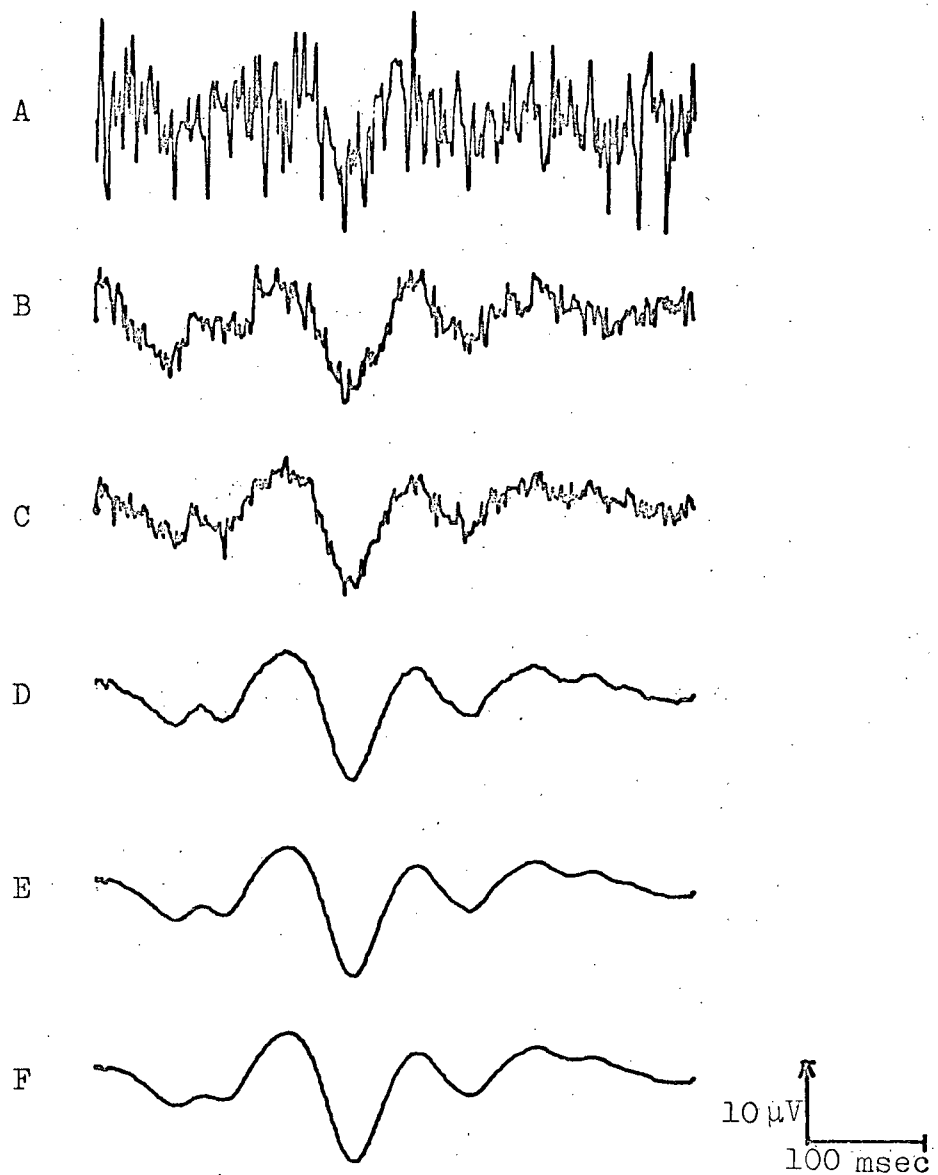


Fig. 2.3.1 The Noise Reduction Process, showing, (a) the single system response, (b) the average of 64 responses, (c) the average of 128 responses, (d) the output from the first application of the sliding mean, (e) the output from the second application of the sliding mean, (f) the output from the third application of the sliding mean.

where $E \left\{ n_z^2(t_i) \right\}$ represents the ensemble mean as before.

It can be seen that the variance of the noise has been further reduced by $1/L$. Hence, one can anticipate an improvement in the signal-to-noise ratio of \sqrt{L} .

The effect of the transformation performed by the sliding mean process can be approximated by a low pass filter with a high frequency cut-off determined by the Nyquist Sampling Theorem. If a 1 second signal is digitized into R discrete values, the maximum frequency component in the digitized signal will be approximately $R/2$ Hz. The maximum frequency component of the output of the sliding mean process will then be approximately $R/2L$ Hz.

A value of ten was chosen for L as a suitable compromise between the noise reduction and the bandwidth reduction of the V.E.P. The effects of the entire noise reduction processing can be seen in Fig. 2.3.1. After the application of the sliding mean, the entire waveform was shifted $L/2$ units to the right in order to preserve the proper latency relationships. It can also be seen, that repeated application of the sliding mean can be performed with little or no alteration of the V.E.P., but virtually complete elimination of the noise.

2.4 Correlation on a Digital Computer

Before proceeding to the experimental portion of the thesis, one further data processing technique warrants discussion at this stage. In the absence of a stimulus input to the visual system of Fig. 2.1.2, the output consists solely of the noise $n(t)$. A potential vs time recording of the spontaneous activity generated within the brain in the absence of any external stimulus input, is referred to

as the Electroencephalogram (E.E.G.). Embedded within this random activity is a spontaneous potential oscillation also generated by the brain at a frequency between 6 and 15 Hz, known as the Alpha Rhythm. The amplitude of the Alpha Rhythm varies considerably between individuals and in time for any one individual.

In Section 2.5, the Alpha frequency is compared with the dominant frequencies of the V.E.P. and their possible relationship is discussed. While the dominant frequencies of the V.E.P. are easily measured from an X-Y recording of the output of the sliding mean or averaging processes, the frequency of the Alpha Rhythm cannot usually be measured in this way. The lack of a stimulus synchronized with the Alpha Rhythm makes the use of the averaging technique difficult if not impossible, and hence, only a single record can be used for measurement. However, since the Alpha Rhythm represents the dominant periodic component of the E.E.G., for most individuals, the Alpha Frequency can often be determined from the time auto-correlogram of the E.E.G.

Assuming $n(t)$ is both zero-mean* and stationary*, the auto-correlation function estimate of $n(t)$ is independent of the time origin, and also is not distorted by the presence of a dc offset in the noise signal. Since the E.E.G. differs from the noise, if at all, only by the presence or absence of the Alpha Rhythm**, which is also zero-mean and reasonably stationary over the half second period during which it is measured, the E.E.G. is assumed to satisfy the theoretical assumptions of zero-mean and stationary behaviour. Also, since the correlation was performed on the digital computer, the

* Both assumptions are investigated in Section 2.6.

** The presence or absence of the Alpha Rhythm in the noise is discussed in Chapter 3.

finite or discrete representation of the correlation function is presented.

Bendat and Piersol⁽¹⁰⁾ provide two digital estimates of the auto-correlation function, the best being defined by the equation

$$\hat{R}_{1x}(\tau) = \frac{1}{N-r} \sum_{i=1}^{N-r} x_i x_{i+r} \quad r=0, 1, 2, \dots, m \quad 2.4.1$$

where x_i represents the signal (E.E.G.) value of the i th sample, N the total number of samples taken, and r , the number of samples in the time delay τ . If the sampling rate was again n samples per second, as in Section 2.3, the delay time is given by $\tau = \frac{r}{n}$. The value of m chosen hence determines the maximum value of τ and cannot exceed N . Although, for $m \ll N$, equation 2.4.1 provides the best estimate of the true auto-correlation function, it was found that in actual practice, as m was increased to values close to N so as to facilitate the accurate measurement of the frequencies of interest, the behaviour of $\hat{R}_{1x}(\tau)$ became erratic and meaningless because of the high noise content of the signal. This phenomenon occurred as the number of samples in the summation decreased to the point where the noise was no longer averaged out sufficiently. To avoid this erratic behaviour of the auto-correlogram, a biased estimate, the second of the two proposed by Bendat and Piersol, was chosen and is defined by the equation

$$\hat{R}_{2x}(\tau) = \frac{1}{N} \sum_{i=1}^{N-r} x_i x_{i+r} \quad r=0, 1, \dots, m \quad 2.4.2$$

where all symbols are as previously defined.

It can be seen that for large r or m , the amplitude will be

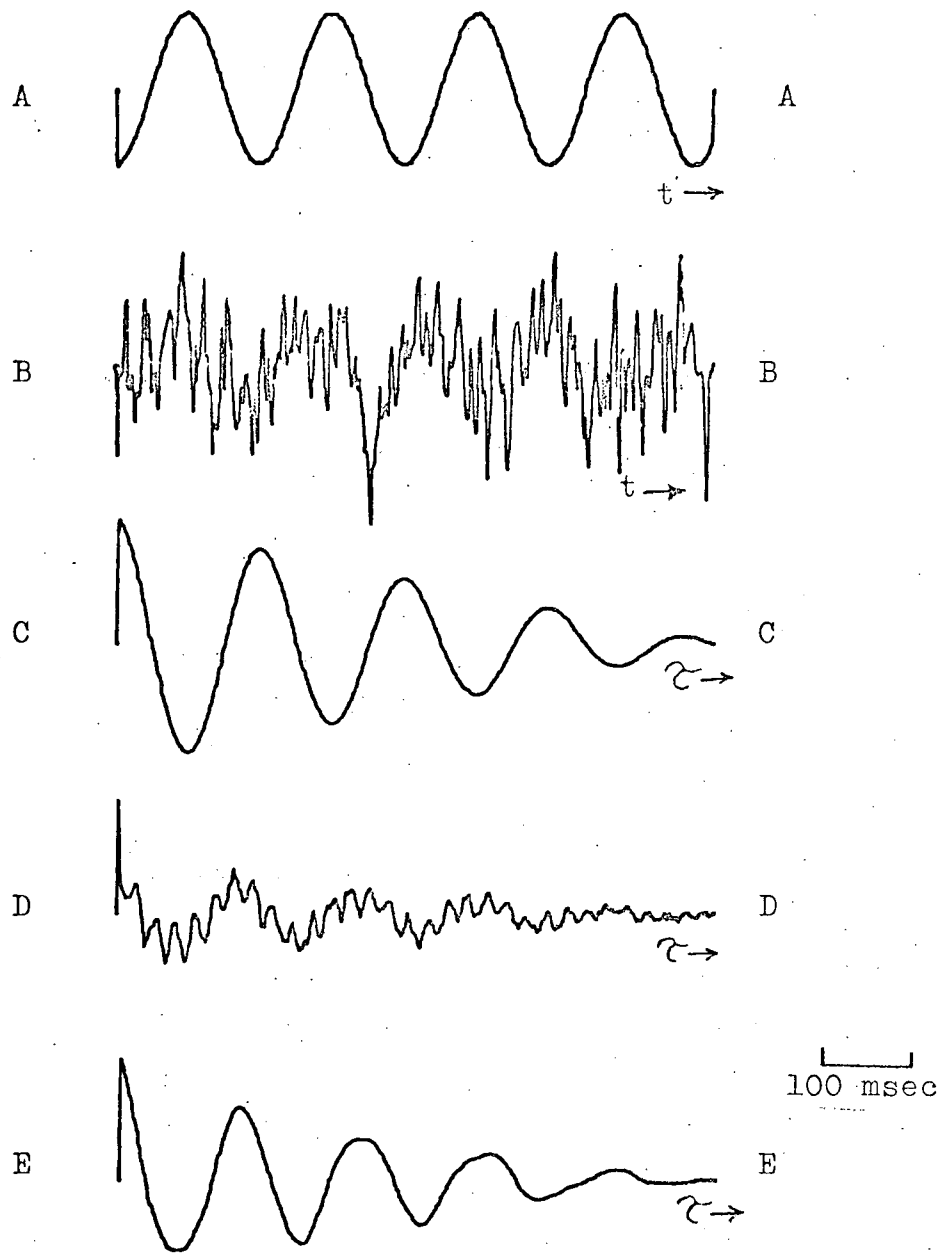


Fig. 2.4.1 Normalized* Auto-Correlogram Estimates showing (a) an 8 Hz. sine wave, (b) An E.E.G. sample, (c) $\hat{R}_{2x}(\tau)$ of the 8 Hz. sine wave, (d) $\hat{R}_{2x}(\tau)$ of the E.E.G., (e) $\hat{R}_{2x}(\tau)$ of the E.E.G. after application of the sliding mean process.

* Auto-correlograms have been normalized to a constant ampl. at $\tau = 0$.

reduced as the divisor N is not decreased with the decreasing number of samples averaged. However, since only the frequencies were of interest, this was not considered to be a serious limitation.

It was found that with this biased estimate, no erratic behaviour occurred and accurate frequency measurements could be made.

Figure 2.4.1 shows a typical E.E.G. and the estimate of the auto-correlogram computed using Equation 2.4.2. To illustrate the actual biasing effect of the estimate, a sine wave and its auto-correlogram are also included.

2.5 The V.E.P. Detection and Processing

A signal flow diagram of the V.E.P. detection and processing equipment is shown in Fig. 2.5.1. The technical information and specification for the major equipment is provided in Appendix I.

At the beginning of an experiment, the subject was seated inside a completely darkened and electrically shielded chamber for a prescribed period of time (see Section 3.1). The shielding was necessary to avoid contamination of the low level ($< 50 \mu\text{V}$) signals by external interference. The stimulus was delivered via a small aperture in the chamber wall directly in front of the subject at eye level, and connections to the electrodes on the subject's scalp were made with shielded cable passing through the chamber wall to the differential amplifiers.

Five scalp electrodes were used in conjunction with four channels of differential amplification. A switching box was designed and built to enable the application of any desired combination of the five electrode signals and a ground into the four channels of the amplifier. Hence both bipolar (one electrode into each input of the

differential amplifier) and monopolar (one electrode on one input and the other input grounded) responses could be examined. The system ground was connected to the lobe of the left ear of the subject.

The four signals from the amplifier were simultaneously recorded on four tracks of an eight-channel F.M. tape recorder and processed by an average response computer. The average response computer performed the ensemble averaging process discussed in Section 2.2. As each light stimulus was presented to the subject, a synchronous pulse was delivered to the average response computer by the electronic stimulator. Triggered by the pulse, the computer sampled each of the four signals from the amplifier simultaneously for a prescribed period of time, usually 500 msec. The computer was set to sample a preset number of responses and display the four ensemble averages on a monitoring oscilloscope. The averaged signals were then plotted on paper using the X-Y recorder.

A logic interface was built to enable data transfer in digital form from the average response computer memory to the off-line PDP-9 digital computer for further processing. The interface, which was controlled by the average response computer, worked in conjunction with a paper tape punch which punched the information on paper tape in a format compatible with the PDP-9 paper tape reader. The circuit diagram and a description of operation for the interface is provided in Appendix II.

In addition to the storage of the ensemble-averaged data on paper tape, it was deemed desirable to store the raw analog data on magnetic tape as it was accumulated. This was often done without the on-line averaging and plotting in order to speed up the experiment and facilitate the accumulation of more data during any one ses-

sion. Also, it was often necessary to re-examine the raw data for transient and artifact interference which often first appeared in the off-line analysis.

As an aid to the cataloguing, recording and playback of the raw data on the magnetic tape, a digital encoding-decoding system was built (see Appendix III). In the recording mode, the encoder was used to generate a unique binary code each time a light stimulus was presented to the subject. This binary code was placed on a fifth track of the tape recorder in "parallel" with the four channels of data. The encoder was triggered by a pulse delivered by the stimulator synchronously with the light flash. This pulse was recorded on a sixth track of the tape recorder. Visual monitoring of the binary code was provided to enable further cataloguing as desired.

On playback, the encoder was used to search out a desired set of data and to start and stop the average response computer processing. The decoder could be preset to detect any particular code desired and to start the averaging process. Visual monitoring of the code as it was examined by the detector was also provided to facilitate the locating of information on the magnetic tape.

An oscilloscope and X-Y recorder were used to monitor the accumulation and processing of data both on and off-line. An I.B.M. 7044 was used in the final stages of the data analysis to perform statistical analysis for the system model of Chapter 4.

Preliminary Data Processing

The signal-to-noise ratio of the visual system as defined in Section 2.1 varies considerably from system to system. As a result, the number of signals required by the ensemble averaging process to reduce the signal-to-noise ratio to a prescribed value also varies

considerably. In order to establish a suitable compromise between time and noise reduction, ensemble averages of from 2 to 1024 signals were investigated and it was found that 128 was satisfactory for most cases. This value was used as a standard number for most of the experiments described in this thesis. The average response computer was also used in the processing of E.E.G.s to measure Alpha frequencies. In the absence of a stimulus, the computer was manually triggered and sampled a desired length of E.E.G. information, converting it to digital form and storing it in memory. The information was then punched onto paper tape for further processing on the PDP-9 computer.

Following the procedure used by most experimenters, ^(1,2,3) a scanning time of 500 msec was chosen as adequate for the complete recording of a V.E.P. Similar lengths of E.E.G. data were generally taken.

As it came from the average response computer, the data contained various artifacts introduced by the detection and averaging processes, which had to be removed or compensated for before further data processing could be applied. The first of these artifacts to be removed was a dc component of unknown magnitude introduced by the average response computer. Since this dc component was impossible to distinguish from physical axial offsets, it was decided to remove all dc from the signal by taking the average value and subtracting it from the signal. This operation was performed on both the V.E.P. and E.E.G., using the PDP-9 computer.

A second artifact in the form of amplitude attenuation was introduced at the scalp-electrode contact. Electrode pressure, the degree of electrode saturation with saline solution, scalp cleanliness,

and hair thickness all influence the impedance of the scalp-electrode contact and hence the amplitude of the response in spite of precautions taken to standardize the electrode mounting procedure. As a result, it was impossible to distinguish between artifact attenuation and amplitude variations due to physiological changes between experiments. For this reason, all signals were normalized on the PDP-9 to a constant RMS value before further processing, except when it was desired to compare responses taken from any one individual during a single experimental session as in the intensity and stimulus size experiments. Otherwise, comparisons in amplitude were made on the basis of an estimate of the signal-to-noise ratio as it would not be affected by attenuation of the overall response either by artifact or amplitude scaling.

Finally, a ten point sliding mean was performed on virtually all of the data according to the procedure outlined in Section 2.3. This resulted in a bandwidth reduction to approximately 25 Hz. The remaining signal, therefore, consisted essentially of the "slow waves" of the V.E.P. The results reported in this thesis are based primarily on the nature of these slow waves.

The sliding mean was sometimes performed on the E.E.G. to enhance the effective "signal-to-noise ratio" of the Alpha Rhythm. This procedure resulted in higher correlation and easier measurement of the Alpha frequency from the auto-correlogram. (see Fig. 2.4.1).

2.6 Experimental Verification of the Theoretical Assumptions of the Model of the Visual System

In Section 2.1, it was assumed that the noise $n(t)$ at the output of the system model was zero-mean, Gaussian and statistically independent of the signal $s(t)$. In Chapter 3, it will be demonstrated

that for a fixed input, $s(t)$ may be regarded as a constant. Under these conditions then, $n(t)$ can be treated as statistically independent of $s(t)$.* The remaining assumptions, however, were left to be proven in this section.

To obtain a sample of the noise $n(t)$, the obvious approach would be to sample the output in the absence of a stimulus input. This output has been previously defined as the E.E.G. However, it has also been noted that the E.E.G. contains a variable periodic component, the Alpha Rhythm, which may or may not be present in the noise $n(t)$ when a stimulus is being applied.** On the possibility that $n(t)$ may change with the application of a stimulus, it was decided to use a single response with a particularly poor signal-to-noise ratio as an approximation to the noise $n(t)$. If the signal-to-noise ratio is particularly poor, the output will differ only slightly from the noise and the difference in statistical properties of the two should be negligible. Since the stimulus rate was usually 1 flash per second, the noise samples added in the averaging process were spaced by 1 second in time, and hence the distribution of noise samples spaced by the same amount is of interest. To obtain such information, the data from a subject with a low signal-to-noise ratio was played into the average response computer. The scanning rate was set as low as possible (1.25 samples per second) to approximate the spacing between samples in a regular recording session. The distribution of the amplitude of these sample observations is shown in Fig. 2.6.1, compared to the Gaussian distribution, along with the mean and variance of the data, and the results of the Chi-square "Goodness of Fit"

* Statistical independence cannot, in general, be assumed.

** The effect of an applied stimulus on the Alpha Rhythm is the subject of much controversy and is discussed in Chapter 3.

test to the Gaussian distribution. The amplitude distribution is shown plotted against the unit normal deviate z . The variable z corresponds to the value of the zero-mean, unit-variance Gaussian random variable for which the probability that a sample observation from the same Gaussian data will be less than or equal to z is equal to the observed fraction of observations which were less than or equal to a given value of the random variable (amplitude) being tested. If the data were perfectly Gaussian distributed, the points would lie in a straight line which would cross the amplitude axis at the mean value and the slope of which would be equal to the inverse of the standard deviation of the data. The Chi-square percent refers to the percentage of sample observation sets from exactly Gaussian data that one would anticipate to have a worse figure for the goodness of fit than the one observed for the data in question. The noise is assumed to be Gaussian distributed on the basis of the results of Figure 2.6.1. It was also found that this mean and variance was approximately constant for any time "origin".

The second major assumption, that of uncorrelated noise samples separated by 1 second in time, is investigated in Figure 2.6.2A. Again, a single evoked response was used as an approximation for the noise $n(t)$. It may be argued that since the noise contains a signal component, it cannot be stationary, but, because of the low signal to noise ratio, this effect is considered negligible. The auto-correlogram of 5 seconds of data is shown in the figure. The noisy behaviour of the correlogram is attributed in part to the fact that the discrete approximation to the auto-correlation function was used and the random behaviour of the signal was not totally eliminated in the correlogram as would be the case in the theoretical

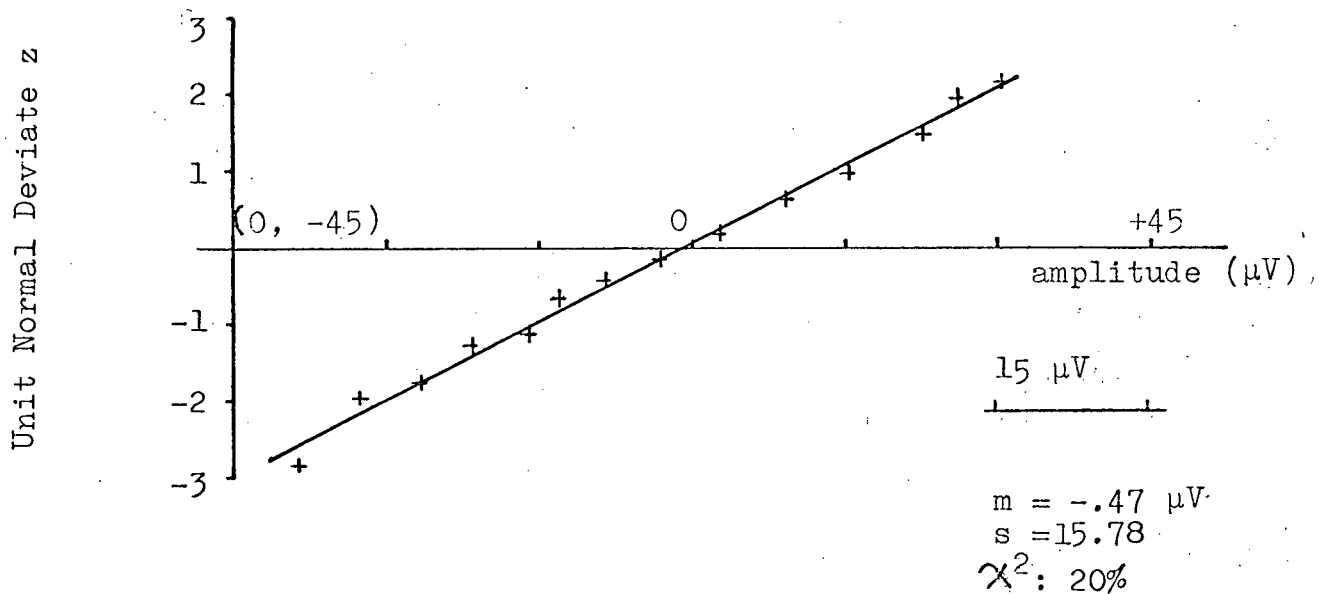


Fig. 2.6.1 The "Goodness of Fit" of the Noise Data to the Gaussian Distribution

limit of an infinite number of samples.

In the theory of the sliding mean, it was assumed that, at a stimulus delivery rate of 1 flash per second, adjacent noise samples were uncorrelated. Since the scanning rate of the computer under these conditions was 500 samples per second, it was in effect assuming that noise samples separated by 2 msec in time were uncorrelated. Figure 2.6.2B shows the auto-correlogram of 50 msec of noise data, the shortest scanning time obtainable on the average response computer. The amount of correlation after 2 msec, (arrow marker), is again submerged in the random fluctuations due to the digital techniques employed.

Since it is impossible to distinguish between the random fluctuations and oscillations due to actual correlation within the data, it must be allowed that some correlation may exist at both time delays of interest. Hence, the results of Sections 2.2 and 2.3

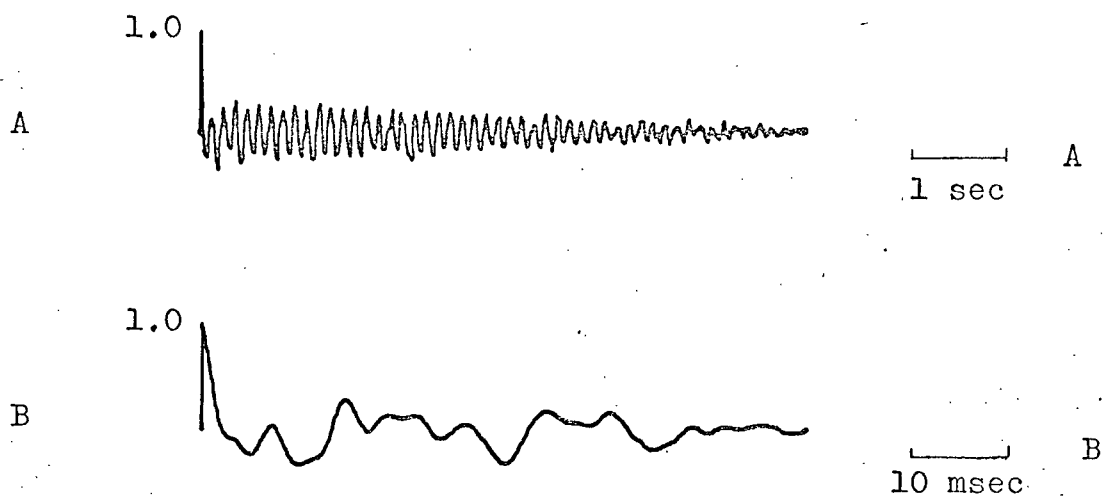


Fig. 2.6.2 Normalized Noise Auto-Correlogram Estimates
 (a) five seconds of the noise $n(t)$,
 (b) fifty milliseconds of the noise $n(t)$.

are only approximate to the extent of this correlation. The presence of correlation would add another term to the final variance equations of these two sections. However, the equations, as they stand, still serve as reasonable approximations to the real situation since the amount of correlation present, if any, is less than that indicated by Figure 2.6.2.

Finally, since the mean and variance of the Gaussian noise are relatively constant over time translations of the "origin", and to the extent that the auto-correlation function of the noise can be approximated by the impulse function, the noise process can be assumed stationary.

3. THE ENVIRONMENT

3.1 Physical Environment

The human Visual Evoked Potential is modified by an unusually large number of influences, both internal and external to the body. The totality of these influences constitute what is defined as the "environment" of the V.E.P.

It could be argued that, as defined (page 4), the visual system must include the entire human nervous system, for, because of the extreme complexity and integrated nature of the nervous system, a small change virtually anywhere in the system could affect every other part of it to a greater or lesser extent. However, most such influences could not be detected with present V.E.P. recording techniques and the effects of the internal variables are largely due to two phenomena; namely, the degree of mental concentration and the general physiological condition of the subject.

Concerning the effects of the general physiological condition of the subject on the V.E.P., little is known. However, the degree of fatigue seems to have some effect on the signal-to-noise ratio of the response, by decreasing the amplitude of the signal component. This effect may be linked with the degree of concentration on the stimulus.

Some work has been done concerning the effect on the V.E.P. of the degree of mental concentration on the stimulus. Garcia-Austt et al.,⁽¹³⁾ have studied the effects of reducing mental concentration, both externally using distraction in the form of small secondary stimuli and internally by assigning a mental task to the subject to be performed during presentation of the stimulus. The results in both cases were reported to be the same -- a reduction in amplitude and decreased consistency of the pattern of the response.

While amplitude variations are partially eliminated in the preliminary data processing procedure as outlined in Section 2.5, pattern variations pose a much more difficult problem.

In the experimental laboratory, the internal environmental variables can be controlled to a limited degree. Subjects can be selected of generally equal physiological condition and a reasonable amount of concentration can be assured. In the clinical atmosphere however, such is not the case. If the V.E.P. is to be used as a clinical tool, allowance must be made for these variations and any model of the V.E.P. which is to be practical must be flexible enough to include these variations within its definition of normality.

In Chapter 4 of this thesis, a statistical model of the V.E.P. is proposed. Since the subjects used in the determination of the parameters of the model were selected at random from the age group 50-80 years, it is proposed that the model will be sufficiently flexible to include the fluctuations due to a wide variation in internal variables. It is felt that subjects within this age group would be capable of less concentration than any other, (with the possible exception of infants), and that physiological variations would be relatively large.

The most important of the external environmental variables include: electrode position, spacing and type; stimulus intensity, duration, size, colour, frequency and background illumination; retinal scotopic or photopic adaptation and site of retinal stimulation--foveal, macular or extra-macular. It is obvious that a description of the V.E.P. which does not include adequate specification of this external environment is of very little value. Much work has been reported concerning the investigation of the effects of varying one or more

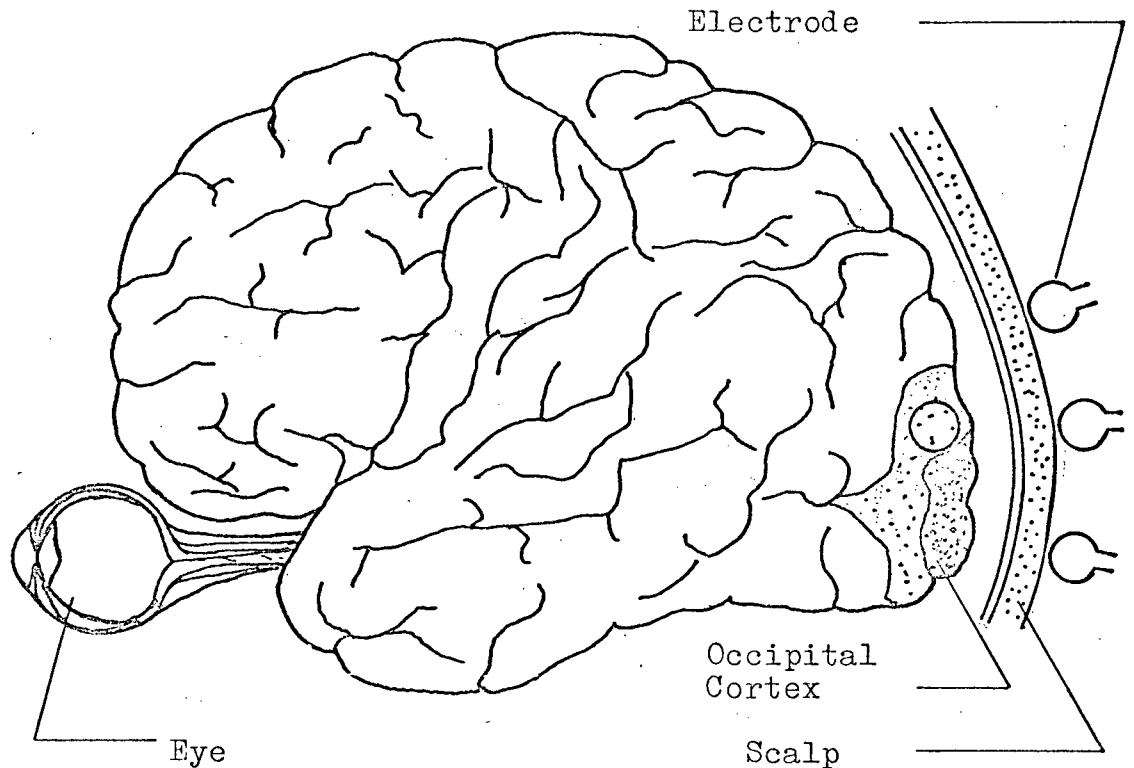


Fig. 3.1.1 The Human Brain, showing the Relation between Electrode Position and the Visual Cortex

of the environmental variables and, where possible, these results have been used. However, several additional preliminary experiments were necessary to investigate the effects of the various parameters and to decide on optimum values for them. In this section, the environment for the model is described in detail and its physiological significance is discussed.

Electrode Placement and Type

The primary region of the brain concerned with vision is called the occipital cortex and is centered under the midline and at the base and back of the skull, as illustrated in Fig. 3.1.1.

The tip of the occipital cortex is indicated externally by a lump on the back of the head, known as the occipital protrusion or

inion. Since this protrusion accurately locates one of the main surface visual centers of the brain, it serves as an excellent reference point for the placing of electrodes to measure visual responses. A preliminary study of the effect of electrode position on the V.E.P. showed that a similar response is obtained over the entire posterior portion of the scalp but that the largest and most consistent responses occurred in the region of the inion. Also, in a study performed by Gastaut et al (13), it was found that some of the short latency components of the V.E.P., in the range 20-100 msec, could be detected only within a few cm of the inion. For these reasons, the work in this thesis was performed with the electrodes on or near the occipital protrusion.

To ensure constant positioning of the electrodes, a small plastic frame was constructed in the form of a cross, with an electrode mounted on each arm and at the center, making a total of five. The distance between the center electrode and any other was 3 cm, and both the frame and electrode shafts were threaded to permit movement of the electrode head toward or away from the scalp as the contour of the skull dictated. The lower electrode was placed directly over the inion and the vertical row of three electrodes was placed along the midline of the head. The approximate position of the electrodes in relation to the visual cortex is illustrated in Fig. 3.1.1. The plastic frame was held in place by an adjustable rubber apparatus and the amplifier leads were clipped on to the ends of the electrode shafts extending above the frame.

Figure 3.1.2 shows the electrodes and mounting apparatus in position. Gold plated, saline sponge electrodes were constructed from center bored brass bolts with concaved heads. The scalp was

cleaned with acetone and the electrode heads soaked with conducting saline solution before placement of the harness. Care was taken to separate the hair from the scalp-electrode contact and each electrode was adjusted to approximately the same pressure. The average inter-electrode dc resistance when in place was about 25,000 ohms.

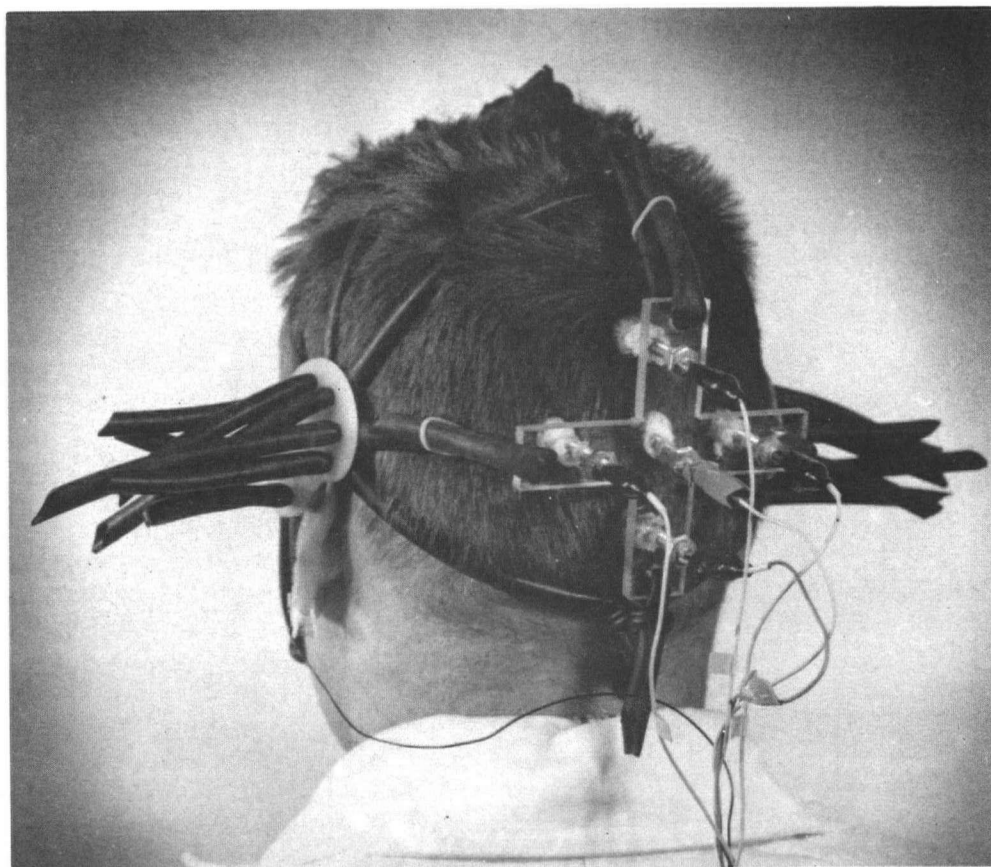


Fig. 3.1.2 Electrode Placement Showing Mounting Apparatus with Electrode Cross and Amplifier Leads in Place

The electrodes were numbered for convenience with number one lying directly over the inion, number two lying three cm immediately above, number three lying three cm to the subject's left of number two, number four lying three cm to the subject's right of

number two and number five lying six cm above number one. Except in a few preliminary experiments, electrode number five was seldom used.

Both bipolar and monopolar responses were examined in detail for the five electrodes positioned as in Fig. 3.1.2. The monopolar responses usually exhibited similar basic patterns with some differences in the amplitude of the major deflections. The monopolar were generally larger and noisier than the bipolar responses. Figure 3.1.3 shows the monopolar responses obtained from electrodes 1 and 2 and the corresponding bipolar response 1,2 taken simultaneously. In the bipolar configuration, the basic pattern of the cortical response is eliminated by the common mode rejection of the differential amplifier. The remaining response is hence the result of the difference between the two monopolar signals and, consequently, local artifacts due to differences in contact impedance and localized noise, which both tend to distort either signal, will be exaggerated in the bipolar recordings. Also, if the five monopolar responses are known, any combination of bipolar responses can be obtained by algebraically subtracting the two monopolar signals concerned on the computer. This is also demonstrated in Fig. 3.1.3. Signal C represents the bipolar response as obtained from the subtraction of the two appropriate monopolar responses. The results are identical as would be expected. For these reasons then, only monopolar responses were recorded and bipolar waveforms were constructed as desired.

The Stimulus

In every experiment described in this thesis, the stimulus was a 10 microsecond pulse of white light provided by a Grass Photo

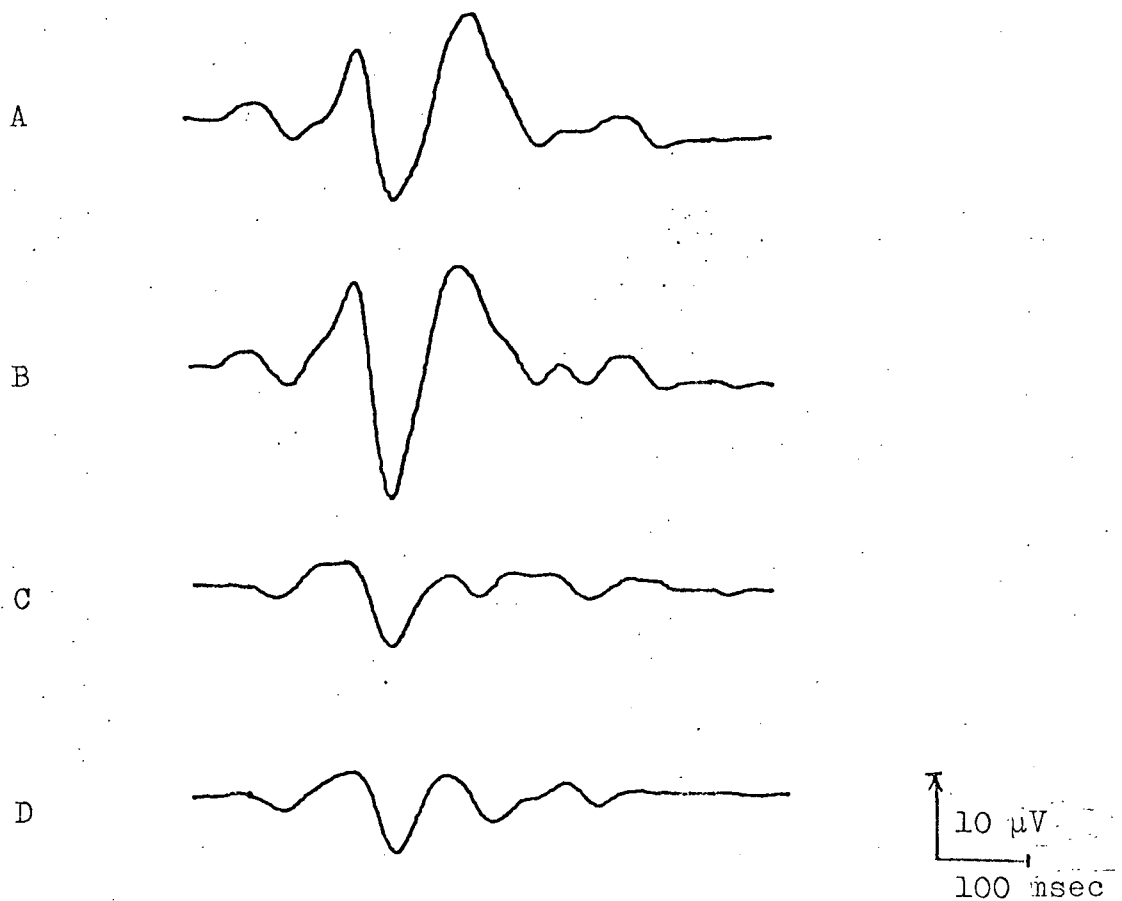


Fig. 3.1.3 Monopolar vs Bipolar Responses
 (a) Monopolar response (1),
 (b) Monopolar response (2),
 (c) Bipolar response (1,2),
 (d) Bipolar response as computed
 by subtracting (1) from (2)

stimulator set at intensity four* and working in conjunction with a standard five inch stroboscope. The face of the stroboscope was covered with a cardboard disc, the center of which had been bored to a prescribed diameter of six millimeters. The subject was seated sixty centimeters directly in front of the stimulus which was at eye level, hence subtending a solid angle about the visual axis of .57

* See Appendix I

degrees at the eye. After ten minutes of dark adaptation, the stimulus was delivered at a rate of one flash per second continuously for the required number of times, most frequently 128. The subject was instructed to relax and sit as still as possible during the course of the experiment and to concentrate on the flash while it was being delivered, with both eyes open. The first five responses were ignored to permit the subject to adjust to the flash intensity and location.

If the V.E.P. is to be used as a clinical diagnostic tool, the relationship between the stimulus parameters and the topography of the eye will be of vital importance in deciding what exactly is implied by a "normal" response and what abnormalities, if any, would be expected to influence the pattern of the V.E.P. For these reasons, a brief description of the retina and occipital cortex is included at this stage and their relationship to the stimulus is discussed.

The Eye and Visual Cortex

The first "stage" of the visual system, the eye, is a complex photoelectric device composed of a large number of each of two types of photoelectric transducers called rods and cones. These transducers are distributed in a non-uniform fashion over the internal posterior portion of the eyeball, under the surface of the retina (see Figure 3.1.4). The rods are the more sensitive of the two detectors, but are not frequency discriminating and hence cannot detect colour. The cones, although less sensitive than rods, have bandpass frequency responses covering one of the three primary colours and hence enable colour distinction. The center surface of the retina, subtending a solid angle of from three to five degrees about the visual axis, is called the fovea and consists of a very dense concentration

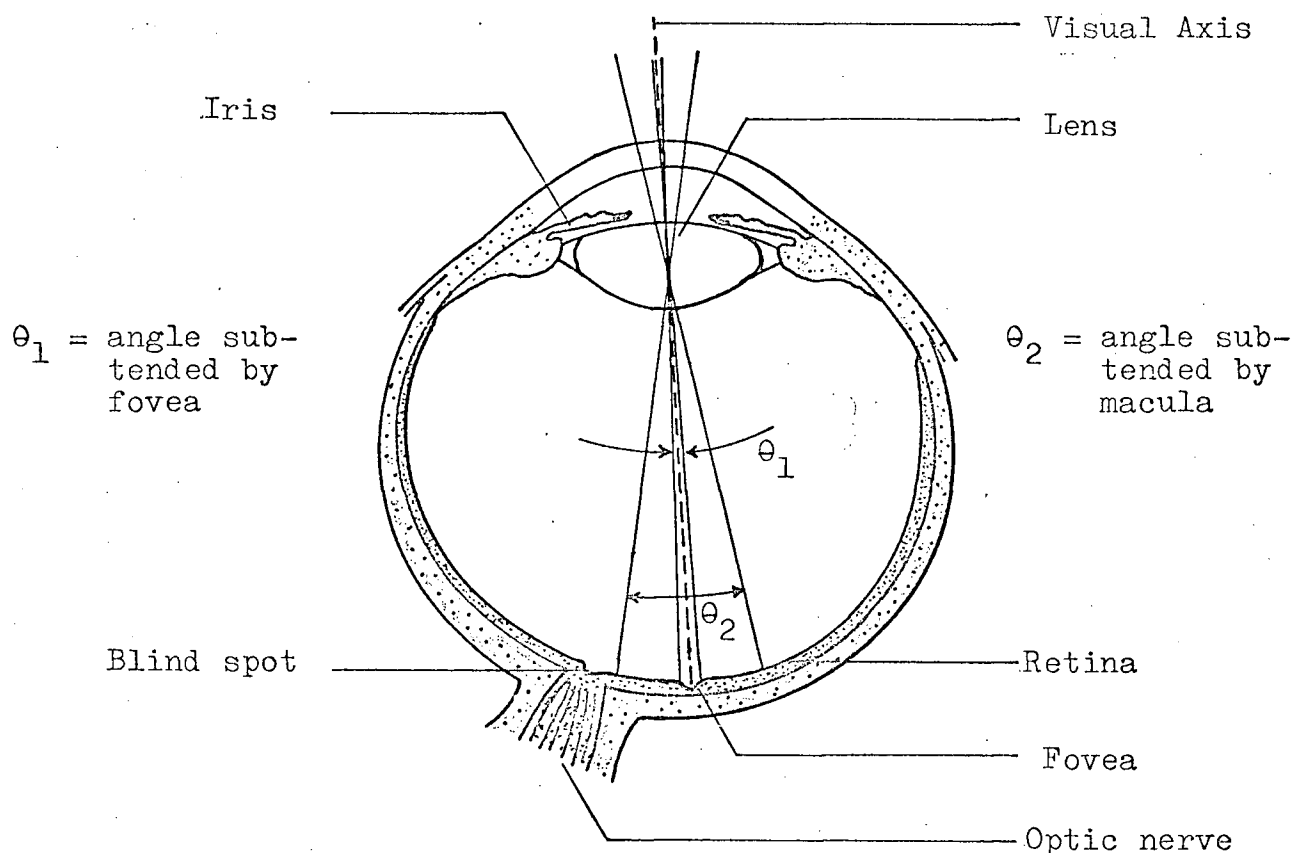


Fig. 3.1.4 The Human Eye, showing Mean Components and Angles Subtended by the Macula and the Fovea

of transducers, almost entirely cones. The fovea is the most frequently used portion of the retina because it is stimulated by objects along the visual axis or in the "line" of vision. Surrounding the fovea is an area of a slightly less dense concentration of transducer cells in general, and a slightly higher proportion of rods in particular. This area is known as the macula and subtends an angle of approximately twenty degrees about the visual axis. The area outside the macula is predominantly rods dispersed in a relatively sparse fashion over the remainder of the retina.

At the level of the visual cortex, physiological experiments have shown that the neural portion of the brain concerned with rod response is located primarily in the medial folds of the occipital lobe, dominating the shaded portion illustrated in Fig. 3.1.1. Since the

largest diameter of stimulus used in any of the experiments subtended an angle of less than two degrees about the visual axis, the largest percentage of stimulated receptors would be cones. For this reason, and because of the topography of the visual cortex, it is probable that the V.E.P. discussed in this thesis is a cone response, specifically the cones of the central fovea.

The localized nature of the stimulus must be borne in mind in any proposed application of the V.E.P. to clinical diagnostics. A "normal" response simply refers to a very small part of the entire system; therefore, a subject with rather severe visual defects in the outer regions of the visual field could conceivably give a "normal" response for foveal stimulation.

Although no experimental investigation of off-foveal stimulation was conducted for this thesis, some work in this area has been reported in the literature. Eason et al, ⁽¹⁴⁾ have examined the response elicited by a red stimulus focused on retinal areas from zero to fifty degrees off the fovea. It was reported that, in general, a good response was obtained in areas up to ten degrees off the fovea, i.e., anywhere in the macular region, but that a decrease in amplitude was observed in the outer off-macular areas. It would therefore appear that any model proposed for the central foveal response could be extended to include the macular region, with corresponding changes in its parameters or form. For this reason, it is not felt that the usefulness of the model proposed in Chapter 4 is limited in its application by the fact that it is based on data provided by foveal responses.

3.2 Linearity and Time-Behaviour of the Visual System

Linearity

Because of the inherent complexity and integrated nature of the visual system, a linear relationship between the stimulus size or intensity and the amplitude or some other characteristic of the response would not be anticipated. Although no such direct linearities have as yet been proposed in the literature, Vaughan⁽⁵⁾ has reported a linear relationship between the latency of some of the major deflections of the V.E.P. and the logarithm of the stimulus intensity.

A preliminary study of the effects on the V.E.P. pattern of varying both the stimulus size and intensity was performed on each of five subjects, male, between the ages of twenty and thirty-five years. The purpose of the study was first to investigate any possible linearities of the visual system for a small stimulus for future experiments -- specifically, for the statistical model of Chapter 4. Fig. 3.2.1 shows the results of a typical experiment in which the stimulus size was varied from .5 mm (2.86 minutes) to 20 mm (1.97 degrees). As can be seen from the figure, the V.E.P. develops in a non-linear fashion from a long latency single major deflection at the smallest size, to the large multideflection responses of the larger stimulus sizes. No attempt was made to determine any logarithmic or other mathematical relationship between the response parameters and stimulus size other than direct linearities. No such direct linearities were found to exist. The transfer function of the system model of Fig. 2.1 is assumed to be non-linear with respect to stimulus size on this basis.

Of primary interest, however, is the fact that there appears to be a "region of immunity" within which the V.E.P. pattern changes

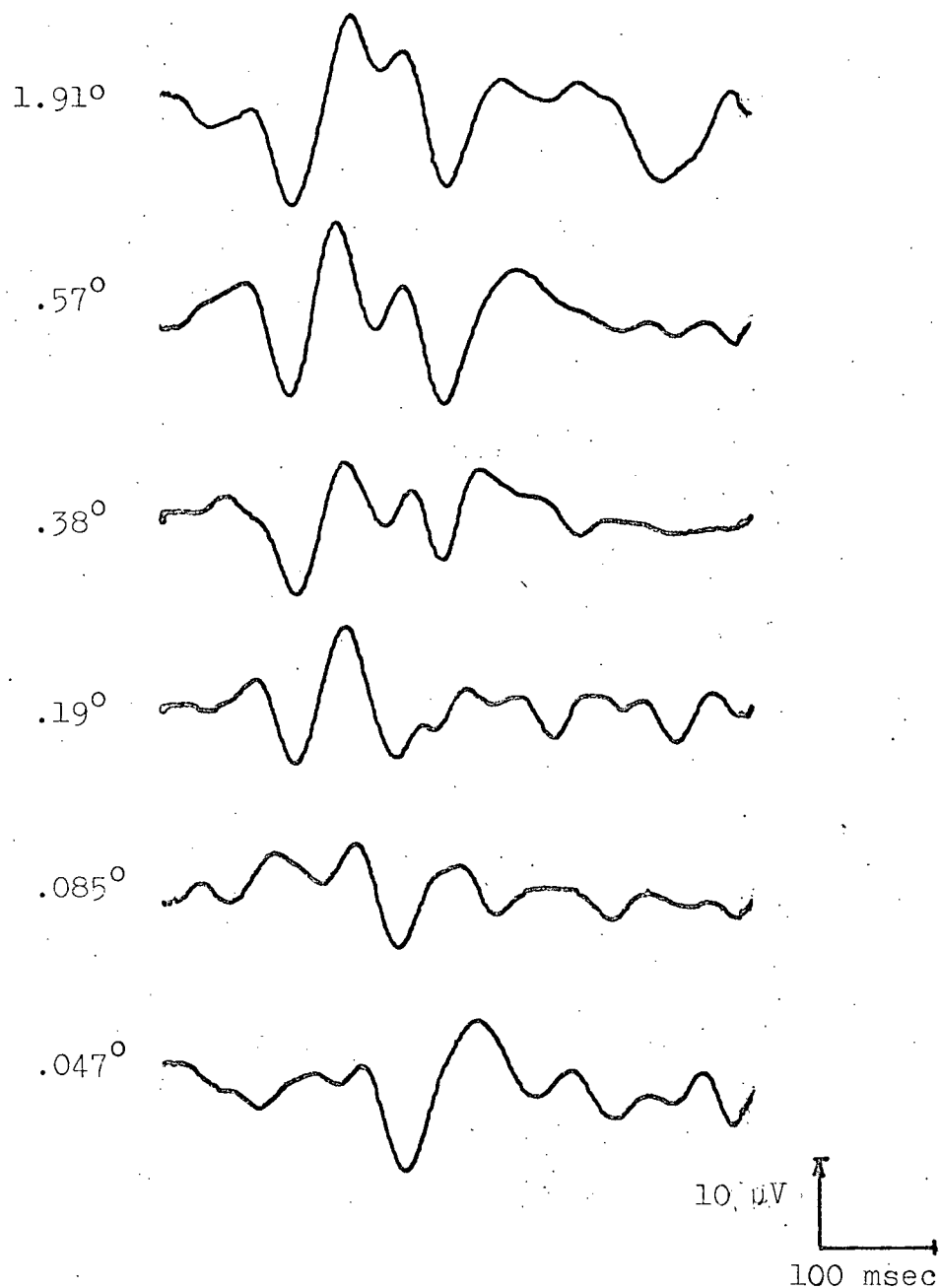


Fig. 3.2.1 The Relation of Stimulus Size to V.E.P. Pattern degrees refer to angle subtended by stimulus perimeter about visual axis.

relatively little with a small change in stimulus size, centering approximately about the .57 degree size. In deciding on an appropriate stimulus size with which to perform the experiments upon which the statistical model of Chapter 4 would be based, it was decided to take advantage of this apparent immunity range. It was felt that if indeed, in this range of stimulus size, the V.E.P. was insensitive to small changes, then it would also be insensitive to variations in individual visual interpretation of the stimulus size. This would partially eliminate one of the physiological variables discussed in the first paragraphs of this section.

The second part of the experiment involved keeping the stimulus size constant at .57 degrees and varying the intensity from 100% of setting four on the Grass photo stimulator,* down to .001% using 10% Kodak neutral density light filters. The results are shown in Fig. 3.2.2. As can be seen again, the V.E.P. appears to follow a non-linear development with stimulus intensity, not dissimilar to that for size. Although the intensity increments and stimulus used by Vaughan⁽⁵⁾ in a similar experiment were different from those used in this experiment, the results appeared similar, particularly at the lower and higher intensities. Again, the pattern appears to vary less at the higher intensities for incremental changes than at the lower values and for the same reasons as outlined for the choice of stimulus size, the larger intensity, 100% of intensity four on the Grass stimulator selector dial, was chosen. Since no direct linearities could be detected, the transfer function $v(t)$ of Fig. 2.1.1 was assumed to be non-linear with respect to stimulus intensity as well. No attempt was made to reproduce Vaughan's logarithmic linearity rela-

* Corresponding intensities in candlepower are provided in Appendix I.

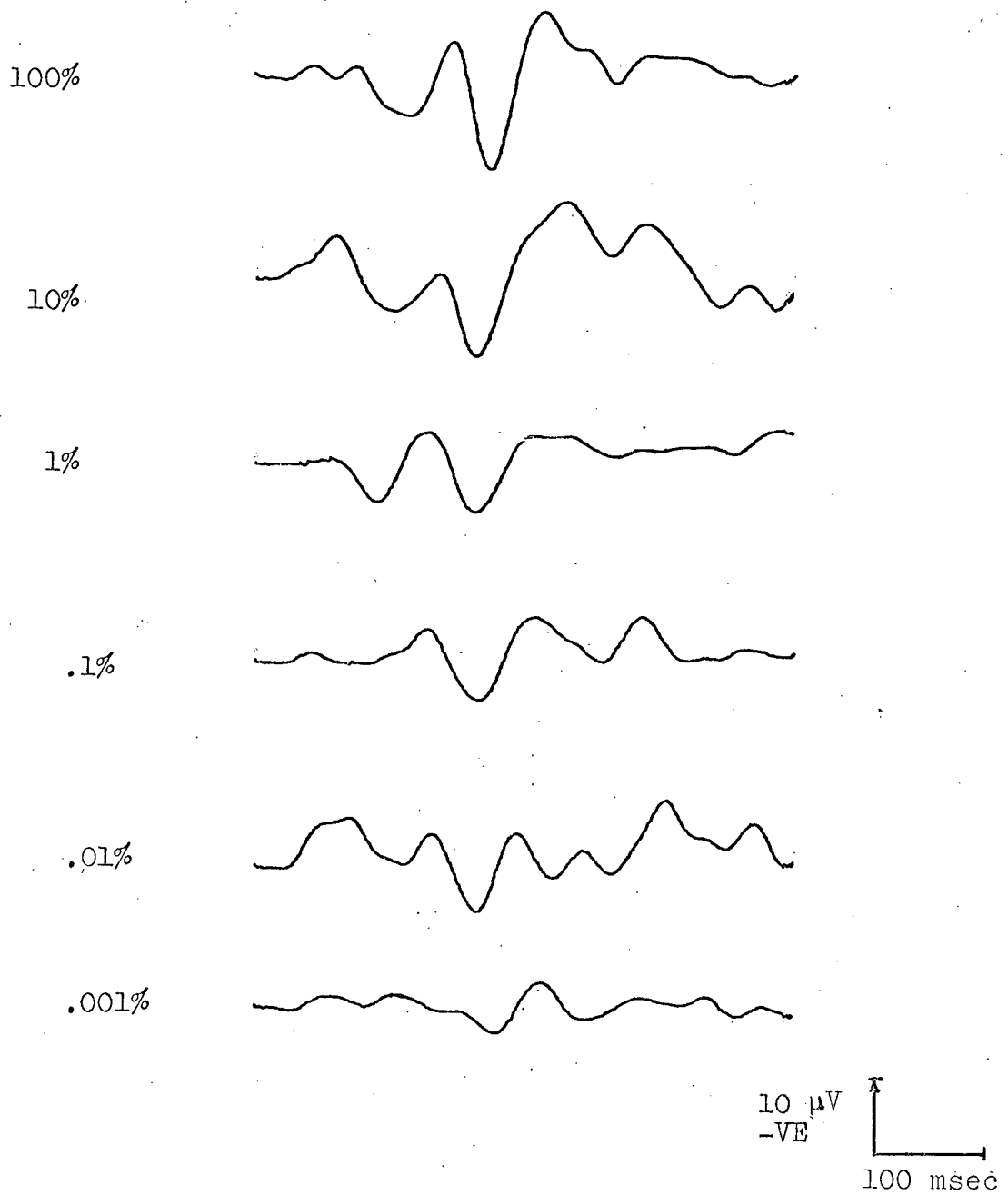


Fig. 3.2.2 The Relation of Stimulus Intensity to V.E.P. Pattern. Percentages refer to % of max. stimulus intensity (setting 4 on Grass stimulator).

tionship between intensity and latency as such linearities would not satisfy the conditions necessary for system linearity.

Time Behaviour of the Visual System

Fundamental to the theory and discussion presented in the previous sections of this thesis is the assumption that the noiseless V.E.P., or some part thereof, is relatively fixed in time and amplitude, or at least normally distributed about some fixed values of time and amplitude. The entire noise reduction process is dependent on the fact that, as the variance of the noisy signal is decreased, the waveform converges to the pattern of the single response. Also, as was pointed out in the introduction to the thesis, the development of a useful model for the V.E.P. depends first on the existence of an individual consistency and secondly on a population consistency in the V.E.P.

The importance of the time behaviour of the visual system necessitated that considerable time be spent in its investigation. While some work has been published in this area, the information provided has been sufficiently vague as to warrant further experimental investigation. Regarding the variability of the V.E.P. both between subjects and over time for any one subject, Wernke and Smith⁽¹⁾ report, "While there was a recognizable similarity between all V.E.P.'s, there were conspicuous departures from the general outline of the response. Those between subjects were outstanding. Less salient were differences between areas of the head and sometimes in an individual when studied repeatedly....The V.E.P. may well serve as a new tool for the study of individuality." Similarly, Rietveld⁽²⁾ reports on a series of tests performed on ten subjects; "The general nature of the response remains generally the same for each one of them. The

degree of this reproducibility is however variable."

Experimentally, five male subjects between the ages 20-35 years were studied over a period of about 10 months and a record of both monopolar and bipolar responses was kept for tests separated by intervals ranging from a few minutes to the full ten months. These records served not only as an indication of the time behaviour of the respective visual systems, but as a check on experimental procedure, artifact interference, and equipment malfunction. Three of the monopolar records are shown in Fig. 3.2.3. As was anticipated from Rietveld's remarks, the consistency does vary slightly from individual to individual. It is of interest to note however, that, while the consistency of the response for any one individual is generally poor when the entire 500 msec is considered, the consistency of approximately the first 250-300 msec is remarkably good. For this reason, one is tempted to subdivide the individual visual response into two components: a relatively time-invariant primary response, and a time-variant secondary after-discharge. Hence, if the model of Fig. 2.1.1 is further restricted to be defined only for the primary portion of the visual response, the transfer function $v(t)$ can be assumed time-invariant for any individual system with little loss of accuracy. This, in effect, is done in Chapter 4 where a statistical model for the visual response is proposed. This subdivision has, in fact, been proposed by other authors and is generally accepted in the literature. The term V.E.P. has frequently been used to refer only to the primary portion of the visual response, while the secondary portion of the response has been termed the "Rhythmic After-discharge". This terminology will be adopted here and used for the

* This does not mean that $v(t)$ is invariant over a set of different individuals.

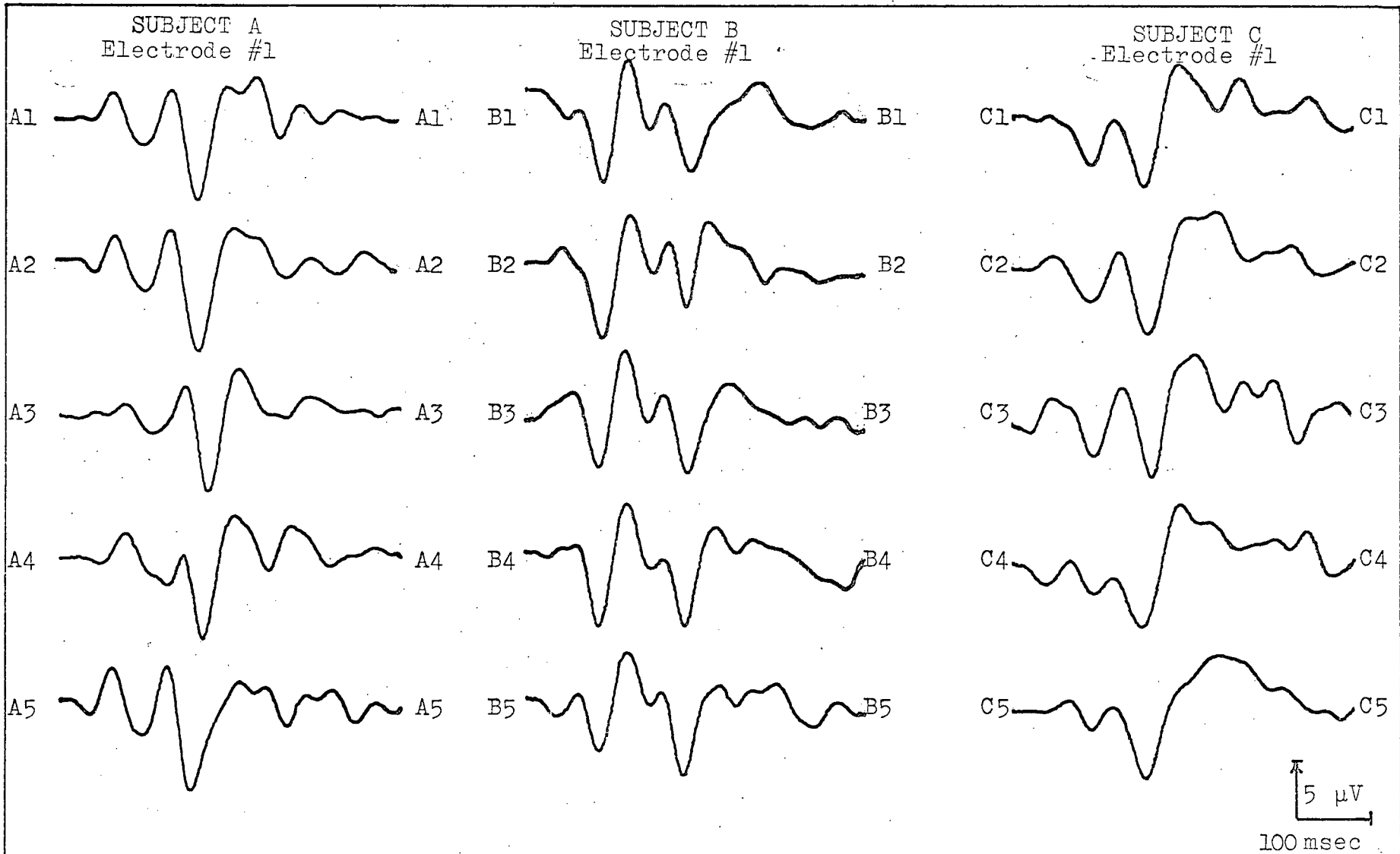


Fig. 3.2.3 Demonstrating the Individual Consistency in Three Subjects Over Ten Months

remainder of this thesis. The term "visual response" shall be used to refer to the V.E.P. together with the Rhythmic After-discharge.

3.3 The Nature of the Visual Response

That a recognizable similarity exists among all visual responses is admitted by most authors; however, the degree of this similarity appears to be somewhat in dispute. It is generally agreed that the visual response consists of two main components as previously discussed -- the V.E.P. which was established as a non-linear time-invariant primary response, and a Rhythmic After-discharge which was described as non-linear and time-variant. These two components are discussed individually in the remainder of this section.

The Visual Evoked Potential

Three approaches to the determination of the nature of the V.E.P. have been described in the literature. Of particular interest are the works of Gazzullo et al.⁽¹⁵⁾, Ciganék⁽³⁾, and Creutzfeld and Kuhnt⁽⁴⁾.

Cazzullo et al have shown that by passing the V.E.P. through two bandpass filters with frequency pass bands of 8-13 and 15-25 Hz , it can be broken up into two main components of a single frequency each. These two components can then be added together to reconstruct the "slow waves" of the V.E.P. with little or no distortion. This result is of interest for the following reasons. First, since selective filtering effectively eliminated the noise*, it would appear to contain no components in the frequency range below 25 Hz. These results also indicate that the V.E.P. is actually the sum of two frequency components, each modulated in an indeterminate fashion, and

* The validity of this statement depends, as in the sliding mean process, on the consistency of the "noiseless" waveform. Good consistency would indicate that the noise had in fact been eliminated, whereas poor consistency would indicate the presence of low frequency noise components.

each lying below the lowest frequency component of the noise. The reason for the success of the sliding mean process can be easily explained in the light of these conclusions. It effectively places a low pass filter on the signal with a cutoff frequency between the lowest noise frequency component and the highest V.E.P. component.

Creutzfeld and Kuhnt have averaged the V.E.P.'s taken from 20 different individuals in an attempt to describe a "mean" V.E.P. The average of 100 responses was taken from each of the 20 subjects and the resulting averaged responses were in turn averaged. The results are reproduced in Fig. 3.3.1A for a monopolar electrode over the occipital cortex. The heavy line indicates the mean waveform and the lighter lines the standard deviation. Because of the deviations in latency of the major deflections observed between individuals -- a fact which is not taken into account in this "average of averages" technique, this mean value is of little practical value and is included only for interest.

The results of a third approach, that taken by Ciganék, are shown reproduced in Fig. 3.3.1B. For this "mean", V.E.P. ensemble averages were taken from 45 subjects and the average values for the latency and amplitude of the main deflections of the V.E.P. were computed. The waveform shown is a sketch of the resulting mean V.E.P. The computed values are provided in table 3.3.1A. This approach is superior to that taken by Creutzfeld and Kuhnt since latency variations are taken into account in the averaging of the amplitudes of corresponding deflection peaks.

As a further investigation into the nature of the V.E.P., a set of experiments was performed in which 50 subjects were examined on a single occasion each under identical environmental conditions.

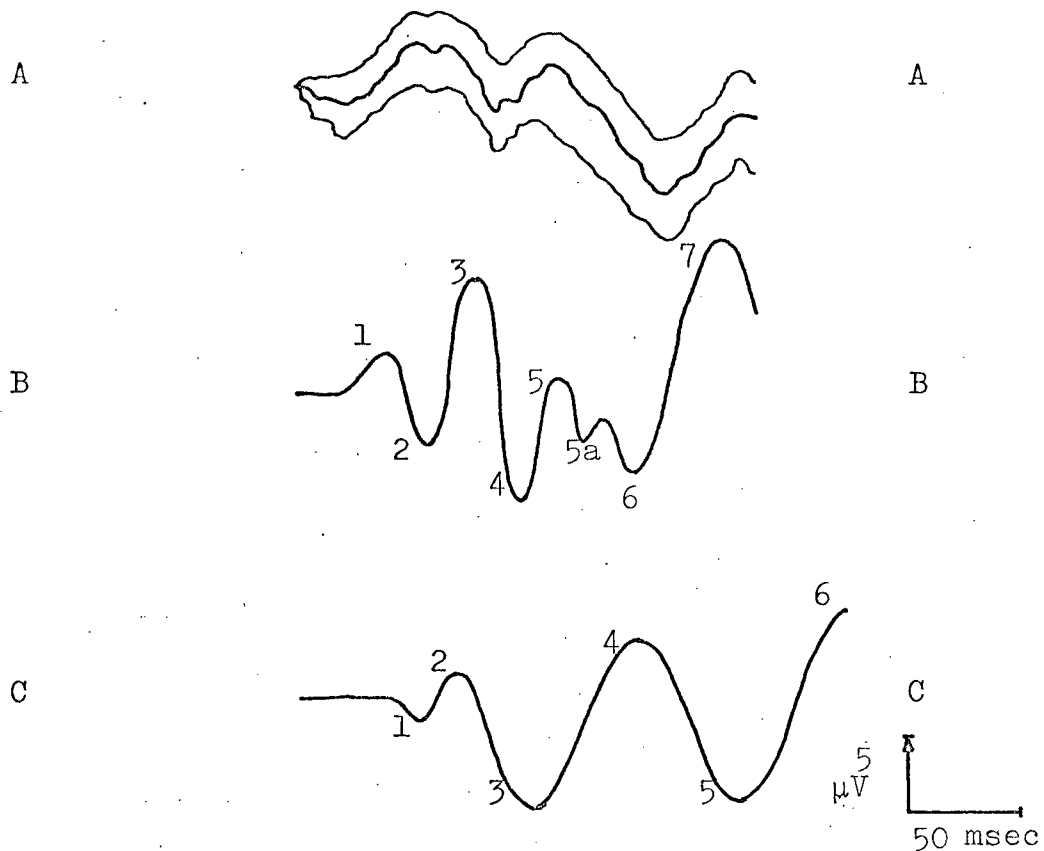


Fig. 3.3.1 Mean Visual Evoked Potentials,
 (a) according to Creutzfeld and Kuhnt,
 (b) according to Ciganék, (c) according
 to Bennett

The subjects, all males, between the ages of 50 and 80 years, were selected at random from the general population of that age group. Typical responses have been selected to show the pattern variations observed and are illustrated in Fig. 3.3.2. The end of the V.E.P. and the beginning of the After-discharge is indicated by an arrow marker in each case. Observing the E.E.G. convention, negativity at the electrode results in an upward deflection on the graph. As each record was taken, an E.E.G. was also recorded for each subject along with the monopolar binocular and monocular responses. On the basis of the fifty individual ensemble averages obtained, a "mean" V.E.P. was computed in the same manner as used by Ciganék. The PDP-9 was used

to scan the slow wave response recording the latency and amplitude of all maxima and minima observed. The mean and standard deviation of corresponding peaks were then computed and are recorded in table 3.3.1B. The waveform sketched on the basis of these calculations is shown in Fig. 3.3.1C. Although a basic similarity exists between the model of Ciganék and that of table 3.3.1B, some notable differences must be explained. Ciganék's deflection number one was not observed with significant frequency and is not included in this new model. Hence, peaks 2-7 in Ciganék's model correspond to peaks 1-6 in the new model. The behaviour which Ciganék had indicated with dotted lines was also observed on occasion but again, not with significant consistency. The two models agree well for the first three deflections, but diverge at the longer latencies. The explanation offered for the discrepancies is that the two environments differed significantly in two critical aspects; namely, stimulus size and intensity. Also, since both models are based on small samples of the population, further sampling may lead to closer agreement of the two results.

Table 3.3.1A Mean Values as Computed by Ciganék

Deflection	1	2	3	4	5	6	7
Latency (msec)	39.12	53.40	78.33	94.19	114.00	134.55	not provided
Standard Dev. (Lat)	4.18	4.42	6.36	7.13	7.41	9.92	
Amplitude (μ V)	2.93	-3.51	5.24	-7.18	.92	-5.52	
Standard Dev. (Amp)	1.59	2.15	3.43	4.18	3.15	2.88	

Table 3.3.1B Mean Values as Computed by Bennett*

Latency (msec)	53.12	67.90	105.41	147.70	194.89	239.02
Standard Dev. (lat)	12.67	15.36	14.78	11.83	20.04	28.51
Amplitude (μ V)	-1.67	1.36	-7.18	4.12	-6.94	5.65
Standard Dev. (Amp)	1.79	2.25	2.56	2.82	3.67	3.25

* The amplitude values have been scaled to the same combined RMS value as those of Ciganék, for comparison, since previous scaling in the data processing procedure had altered the true amplitude.

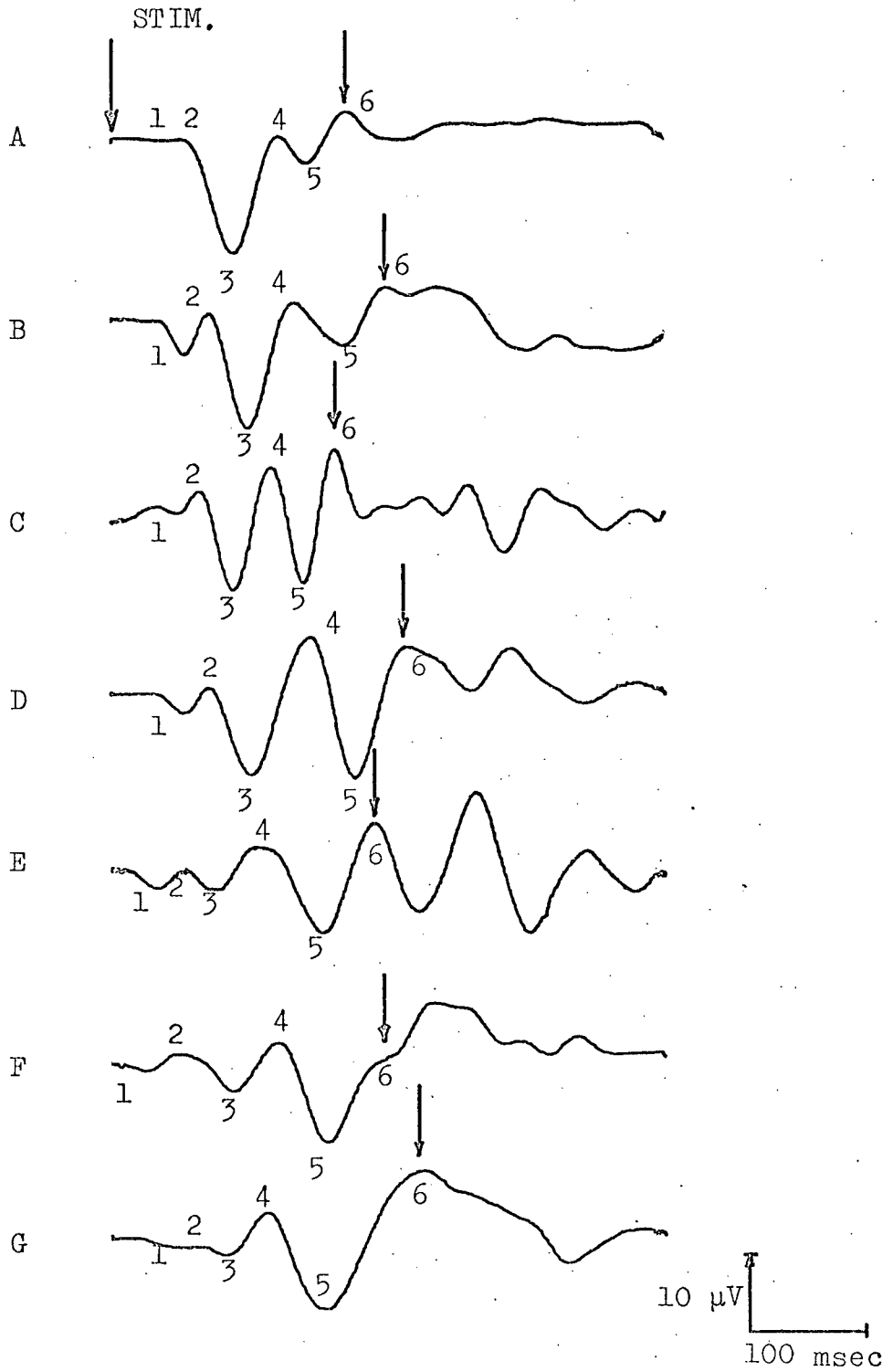


Fig. 3.3.2 Sample Visual Responses

The Rhythmic After-Discharge

Because of the erratic time behaviour of the After-discharge, it has received little attention in the literature and will be discussed only briefly here. However, some work has been done by Rémond et al. (16), investigating the variations in the visual response, specifically the Rhythmic After-discharge, with the phase of the Alpha Rhythm at the time of arrival of the stimulus at the retina. It was found that if the stimulus reached the retina at the time of a maximum in the Alpha Rhythm, the rhythmic activity of the After-discharge was severely attenuated. Conversely, if the stimulus was applied at a minimum of the Alpha Rhythm, this rhythmic activity was strongly amplified. It was also reported that the frequency of this Rhythmic activity was the same as that of the resting Alpha Rhythm.

This latter relationship has also been investigated by Barlow (17), who also reported that an apparent relationship existed between the two frequencies. To verify this proposed relationship, an E.E.G. record was taken for each of the subjects in the sample study previously discussed. The Alpha frequency was measured from the auto-correlogram of the E.E.G. and compared with the frequency of the After-discharge in cases where a measureable oscillation existed. The results are shown in the Table 3.1.2. No attempt was made to determine a relationship between the time of stimulus delivery with respect to the Alpha Rhythm phase and the magnitude of rhythmic activity in the After-discharge. However, as can be seen in the table, the two frequencies appear to be about the same and hence, in part support the conclusions of Rémond et al. Finally, a further piece of evidence was noted in the E.E.G. auto-correlation experiment which further substantiates the hypothesis that the After-discharge is a

resumption of spontaneous activity. In some cases, where a particular subject demonstrated dominant "fast", or high frequency activity in the E.E.G., oscillations of approximately the same frequency were noted in the After-discharge; a phenomenon which would be expected if indeed the After-discharge was a resumption of the spontaneous E.E.G. activity. Examples of the high frequency activity can be seen in Figure 3.3.2C and 3.3.2F, and table 3.3.2. Amplified Alpha activity is demonstrated in responses D and E of the figure 3.3.2, and suppressed activity in responses A, B and G.

For clarification of terminology, the implications of the conclusions of this section must be considered in relation to the definition of the V.E.P. and the system model proposed in Chapter 2. Although the pattern of the After-discharge is related to the stimulus, it cannot be said that the two are synchronized, therefore the After-discharge is not included in our definition of the V.E.P. The signal portion of the output of the system model is hence the V.E.P. alone; a fact which, although not pointed out until now, does not in any way alter the validity of the previous discussion.

After-discharge Hz	Alpha Rhythm Hz	After-discharge Hz	Alpha Rhythm Hz
10.35	10.95	10.90	10.00
9.83	10.05	12.00	12.85
10.30	11.00	22.20	21.25
6.86	5.86	24.00	25.05
8.71	8.75	25.08	24.05
10.40	9.20		

Table 3.3.2 Comparison of E.E.G. Frequencies with Those of the After-Discharge

4. A STATISTICAL MODEL FOR THE V.E.P.

4.1 The Distribution of the Data

As was stated in Section 3.2, it is generally agreed that a recognizable similarity exists among V.E.P.s taken from several different subjects. This would be anticipated from physiological considerations of the human visual system; for while visual experience and learning may differ widely among individuals, the general structure of all visual systems is the same, and each person "sees" essentially the same pattern when an identical object is presented for examination.*

Furthermore, as was also discussed in Section 3.2, some V.E.P. investigators have computed mean values for the V.E.P. by averaging several responses in various ways. These sample means were reproduced and discussed according to their relative merits and agreement in that section.

Except for the reporting of means and variances of the data, no definition or description of the distribution of the V.E.P. pattern has as yet been published. The advantages of such knowledge would be manifold and are discussed in detail at the end of this section. This distribution is investigated following a brief examination of the dependency of the response on electrode position.

Variations in the Mean V.E.P. with Electrode Position

On the basis of the fifty sample responses obtained in the study of Section 3.3, a model for the mean V.E.P. was proposed. This model was obtained by computing the average values of both the latency and amplitude of the constant major deflections observed. For purposes of comparison, the mean V.E.P. reported was for samples obtained

* This is not to say that the interpretation of the object "seen" will be the same for each individual.

from electrode number one located over the occipital protrusion, since the other two models were based on occipital responses. The mean and variance for this electrode and those of the other three are listed in Table 4.1.1. As can be seen from the table, the V.E.P. pattern varies slightly with electrode position. The latency is larger for corresponding deflections for the peripheral responses than for the occipital response. It can also be seen that the relative amplitude of the major deflections of the peripheral responses are essentially the same but differ from those of the occipital pole and radiates outward to the peripheral areas, with some time delay and pattern alteration.

LATENCY (Msec)							
Electrode		Deflection					
		1	2	3	4	5	6
1.	Latency	49.82	66.11	105.00	143.81	190.09	232.09
	Std. Dev.	12.15	14.17	11.31	13.58	20.43	32.01
2.	Latency	49.02	66.44	108.14	146.67	196.04	245.63
	Std. Dev.	12.38	14.64	8.98	13.44	19.83	28.51
3.	Latency	53.12	67.90	107.95	147.93	194.89	238.87
	Std. Dev.	12.67	15.36	9.17	11.23	20.04	33.04
4.	Latency	52.50	67.34	105.41	147.70	194.17	239.02
	Std. Dev.	14.77	15.78	14.78	14.01	20.72	31.78
AMPLITUDE (Normalized μV)							
Electrode		Deflection					
		1	2	3	4	5	6
1.	Amplitude	-1.79	1.86	-8.38	4.68	-6.23	5.27
	Std. Dev.	2.17	2.31	3.17	2.82	4.11	3.47
2.	Amplitude	-1.12	2.01	-7.35	4.64	-8.81	5.45
	Std. Dev.	1.63	2.26	3.20	2.67	3.59	2.98
3.	Amplitude	-1.68	2.41	-7.50	5.25	-7.58	5.47
	Std. Dev.	2.23	2.08	2.91	2.64	3.13	3.40
4.	Amplitude	-1.86	1.53	-8.04	4.61	-7.78	6.38
	Std. Dev.	1.92	2.52	2.87	3.19	4.11	3.77

Table 4.1.1 Comparison of the Latency and Amplitude of the Major Deflections of the Four Electrode Positions

Distribution of the V.E.P. Parameters

The V.E.P. has been characterized by six major deflections,

each of which can in turn be specified by two parameters; the time delay or latency between the time of delivery of the stimulus and the arrival of the maximum point of the deflection, and the amplitude of that maximum. In total, therefore, twelve parameters completely specify the V.E.P. The distribution of these twelve parameters was investigated experimentally using the fifty sample responses obtained in the experiment described in Section 3.1.

On consideration of the physiological and experimental evidence discussed in previous sections, one is tempted to regard the V.E.P. as a random process with some mean value and standard deviation, and as showing some central tendency or clustering about that mean. Since this type of behaviour in nature is often best approximated by the Normal or Gaussian distribution function, the distribution of the data was compared with the Gaussian distribution. To this end, a data histogram was plotted superimposed on the corresponding "modified" Gaussian density function curve, computed using the sample mean and variance for each of the parameters of the four responses. The expression "modified" is used to distinguish between the ordinary probability density curve, and that computed by multiplying this standard curve by the width of the histogram "bins", thus ensuring proper scaling for true comparison. Each of the twelve parameters for the four electrodes was examined in this way. The "goodness of fit" of the data to the theoretical curve was measured using the standard χ^2 Goodness of Fit test, the results of which are illustrated in Table 4.1.2. As in Section 2.6, the χ^2 percentage figure is an estimation of the percentage of sample observation sets taken from exactly Gaussian data which one would anticipate as having a poorer figure for the "goodness of fit" than that calculated for the data in question.

On the basis of these test results, the data cannot be rejected as being non-Gaussian.

As visual indication of the fit of the data to the Gaussian curve, the data for both the amplitude and latency parameters are plotted vs the unit normal deviate* for electrode number one, in Figures 4.1.1 and 4.1.2, respectively. Since the data fits closely to the theoretical curve, and since the χ^2 test failed to reject our hypothesis, the data is assumed to be Gaussian distributed.

		χ^2 Percentages					
		Deflection					
Electrode		1	2	3	4	5	6
1	Amplitude	48	26	62	84	78	84
	Latency	86	87	38	63	84	10
2	Amplitude	60	8	26	60	30	74
	Latency	10	22	35	46	88	31
3	Amplitude	5	18	55	98	10	41
	Latency	10	70	92	88	66	7
4	Amplitude	70	4	9	85	87	77
	Latency	92	73	18	25	86	45

Table 4.1.2 χ^2 Goodness of Fit Test Results

Statistical Model for the V.E.P.

It has been shown that the essential information in the V.E.P. can be specified by twelve parameters which correspond to the latency and amplitude of each of the six peak deflections in the response. It has also been demonstrated that the Gaussian distribution curve with mean and variance estimates as computed from the averages of the fifty sample subject responses represents a good approximation to the actual distribution of the data. Since each peak deflection is characterized by the distribution of two parameters, or random variables, a two-dimensional joint Gaussian density function can be

* See Section 2.6.

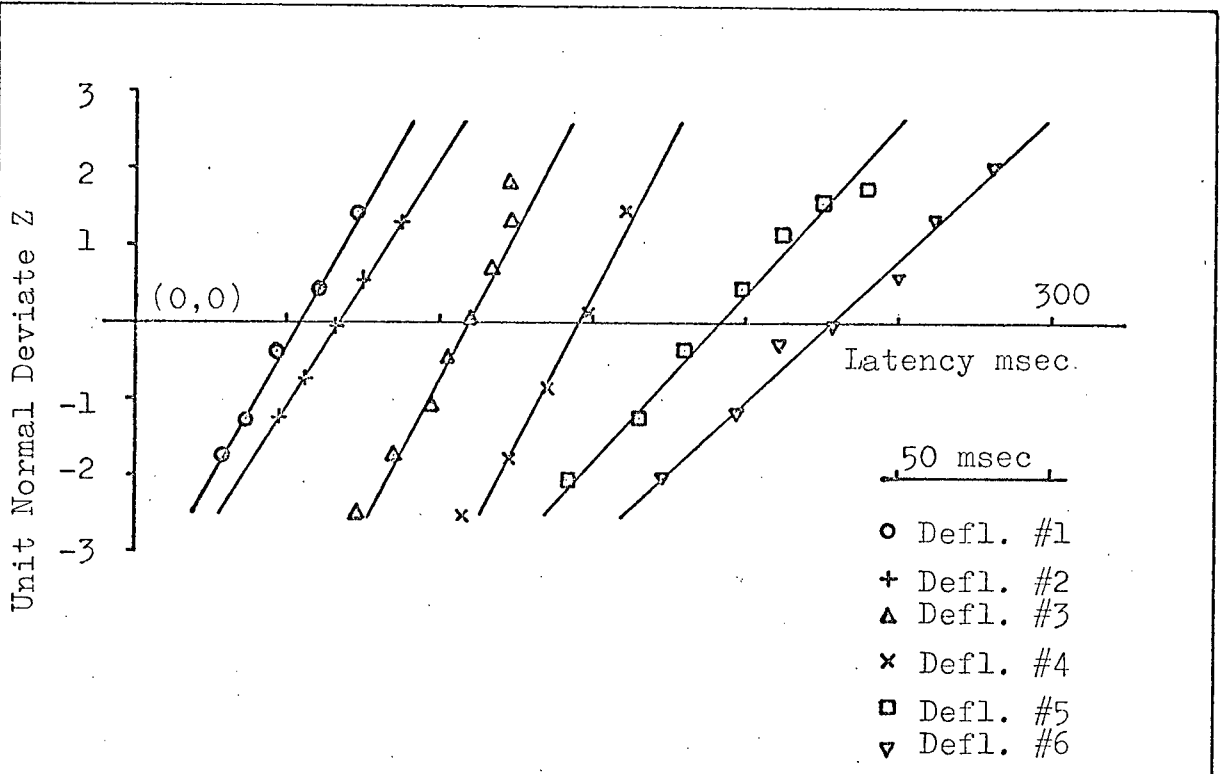


Fig. 4.1.1 Goodness of Fit of the Latency of Electrode Number One to the Gaussian Distribution

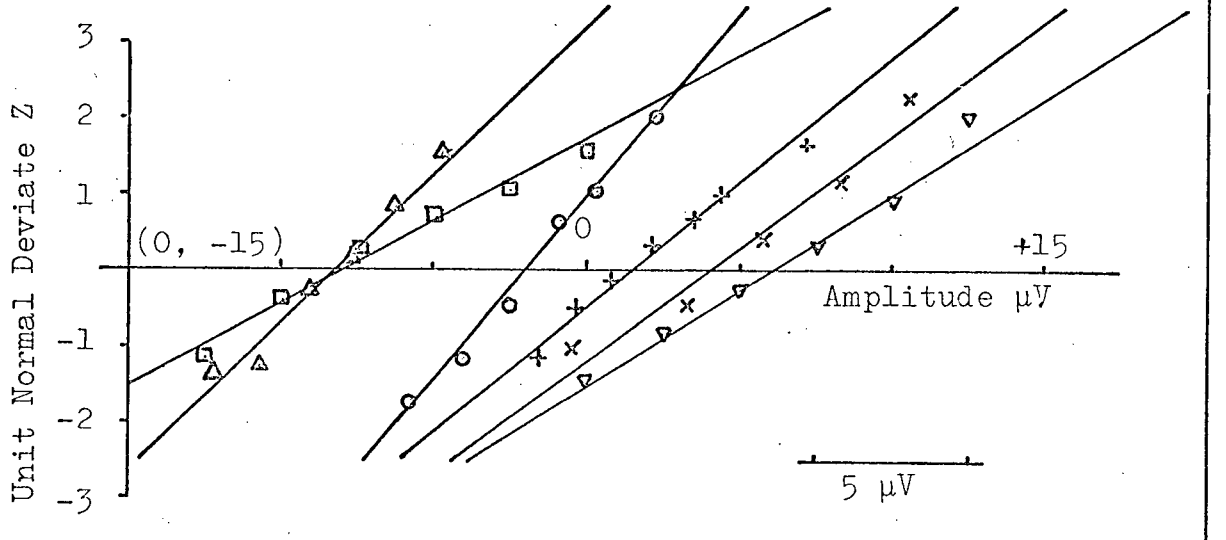


Fig. 4.1.2 Goodness of Fit of the Amplitude of Electrode Number One to the Gaussian Distribution

defined for each deflection maximum, and will be of the form

$$P_{x_1 x_2}(\alpha_{L1}, \alpha_{A1}) = \frac{1}{2\pi S_{L1} S_{A1}} e^{-\frac{(\alpha_{L1} - m_{L1})^2}{2S_{L1}^2}} \cdot e^{-\frac{(\alpha_{A1} - m_{A1})^2}{2S_{A1}^2}} \quad 4.1.1$$

where $P_{x_1 x_2}(\alpha_{L1}, \alpha_{A1})$ defines the probability density for sample observations of the two parameters represented by $(\alpha_{L1}, \alpha_{A1})$ on the latency vs amplitude plane. M_{L1} and S_{L1} represent the mean and variance estimates of the latency of peak one and M_{A1} and S_{A1} , the mean and variance of the amplitude.

By taking the natural logarithm of both sides of the equation 4.1.1 we have

$$\left(\frac{\alpha_{L1} - m_{L1}}{S_{L1}}\right)^2 + \left(\frac{\alpha_{A1} - m_{A1}}{S_{A1}}\right)^2 = -2\text{LN}(2\pi S_{L1} S_{A1} P_{x_1 x_2}(\alpha_{L1}, \alpha_{A1})), \quad 4.1.2$$

which is the equation of an ellipse with center at (m_{L1}, m_{A1}) on the amplitude-latency plane, and semi-axes $S_{L1} \sqrt{-2\text{LN}(2\pi S_{L1} S_{A1} P_{x_1 x_2}(\alpha_{L1}, \alpha_{A1}))}$ and $S_{A1} \sqrt{-2\text{LN}(2\pi S_{L1} S_{A1} P_{x_1 x_2}(\alpha_{L1}, \alpha_{A1}))}$.

Using the Gaussian distribution tables, a value for $P_{x_1 x_2}(\alpha_{L1}, \alpha_{A1})$ can be computed and an ellipse drawn according to Equation 4.1.2. The value of $P_{x_1 x_2}(\alpha_{L1}, \alpha_{A1})$ can be chosen to ensure that a prescribed percentage of observations of $(\alpha_{L1}, \alpha_{A1})$ which define a point on the same plane, will lie within the area enclosed by this ellipse. This area is referred to as the region of acceptance of $(\alpha_{L1}, \alpha_{A1})$ and can be computed for each of the deflections of the V.E.P., enabling the assesment of the total acceptability of a given V.E.P. The acceptability schemes for each of the four electrodes are shown

* Statistical independence of amplitude and latency has been assumed here. While strictly speaking, this assumption has not been verified experimentally, no correlation was detected by visual inspection.

in Figures 4.1.2 - 4.1.6 as drawn by the I.B.M. 7044 computer. The elliptical areas are drawn for the 95% confidence limits in each case, i.e., one would anticipate 95% of normal responses (α_{L1}, α_{A1}) to lie within the elliptical areas.

The statistical models of figures 4.1.2 - 4.1.6, being based only on the fifty observations of the sets (α_{L1}, α_{A1}), are not adequate in their present state for pathological or even experimental application. They are proposed merely as a demonstration of a technique which could be used to build a much more refined model based on several hundred observations, (α_{L1}, α_{A1}). However, as an illustration of an application of the model, two subjects were examined and the observations (α_{L1}, α_{A1}) plotted for each subject on each of the four acceptability schemes of Figures 4.1.2 - 4.1.6. The first subject, male, age 61, was known to have normal vision and the parameters of his response are mapped as crosses on the corresponding schemes. As can be seen, the response is accepted as normal by all four schemes. The second subject, also male, age 82, was known to have advanced Glaucoma and his responses are shown mapped as x's. The acceptability schemes reject the responses as non-normal primarily on the basis of the first two deflections.

While these results are not in any way conclusive, they do indicate that some sensitivity to visual "abnormality" can be anticipated in the model and that further refinement of it may provide a useful experimental and diagnostic tool.

Discussion and Proposals

A preliminary statistical model for the normal V.E.P. has been proposed for each of the four electrode positions on the scalp.

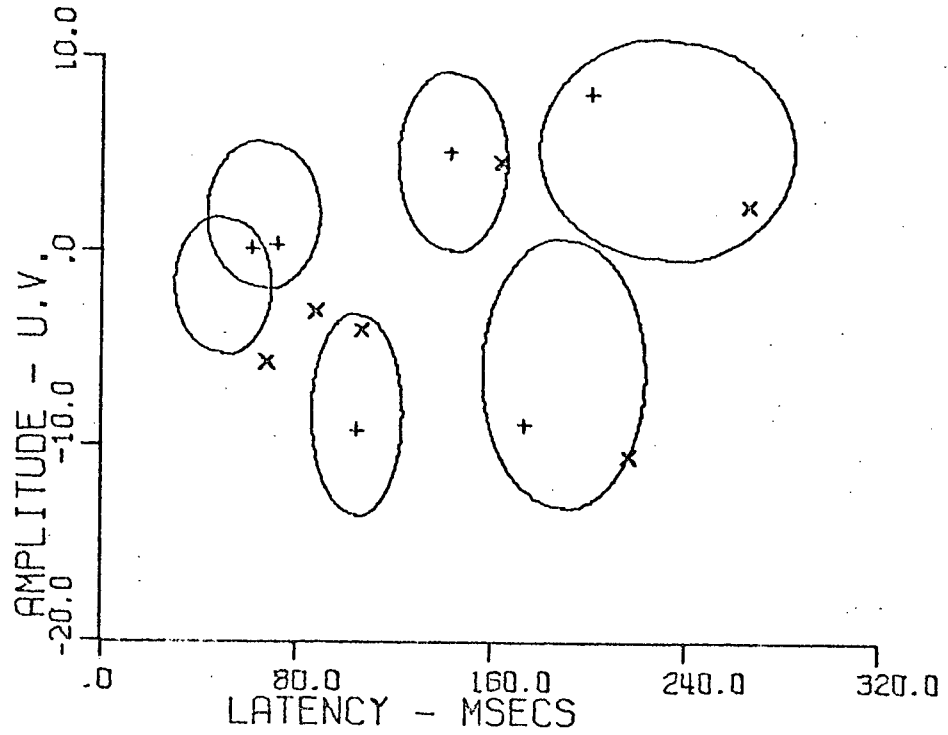


Fig. 4.1.3 Acceptability Scheme for Electrode Number One

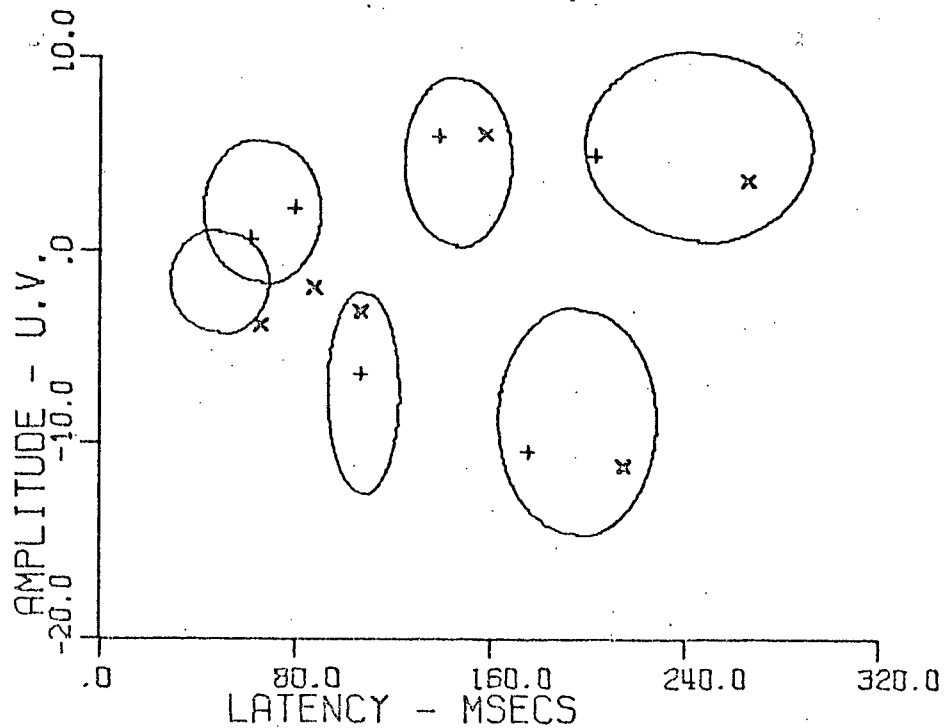


Fig. 4.1.4 Acceptability Scheme for Electrode Number Two

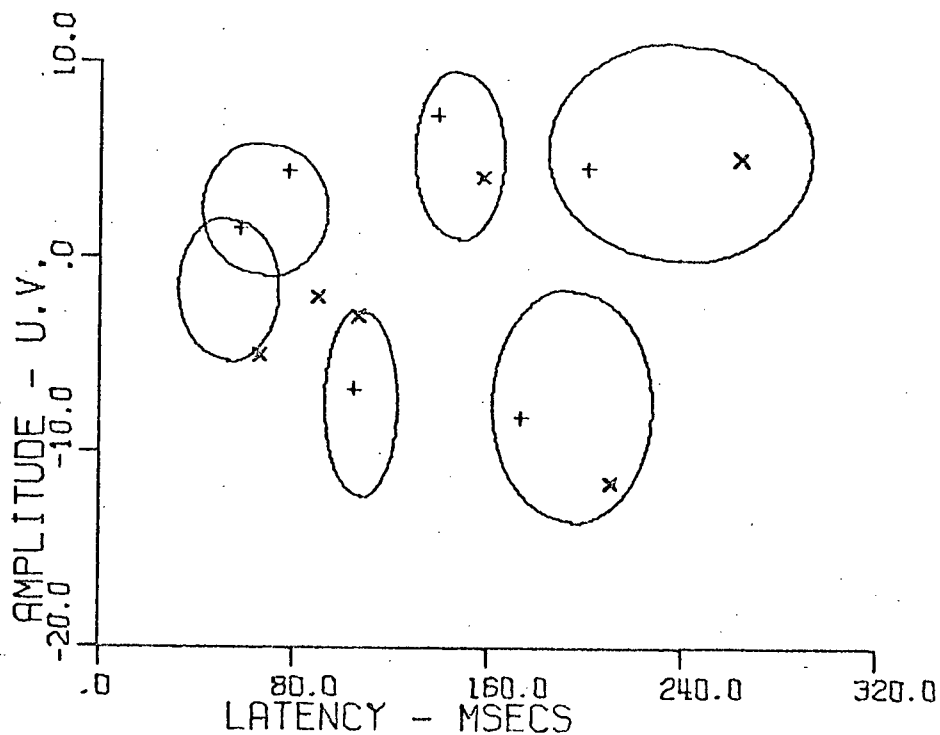


Fig. 4.1.5 Acceptability Scheme for Electrode Number Three

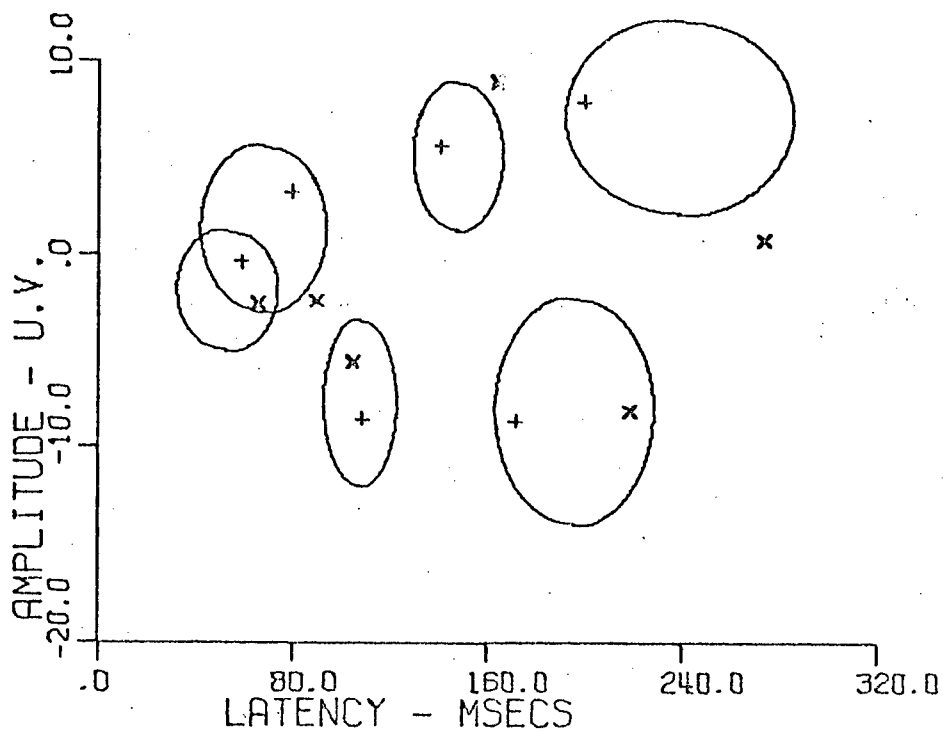


Fig. 4.1.6 Acceptability Scheme for Electrode Number Four

Before such a model could be used to advantage either experimentally or clinically, further refinement of its parameters would be necessary. To this end, the following procedure is proposed.

First, a computer could be programmed to compute and display simultaneously the four acceptability schemes (one for each electrode) on a visual monitoring device. As each new normal subject is examined, the four responses would be fed into the computer, the preliminary data processing of Section 2.5 performed, and the four slow wave responses displayed superimposed on their respective acceptability schemes. The four waveforms could then be inspected for artifact distortion and acceptability either by the computer or the operator on the basis of the "goodness of fit" of the sample to the statistical averages. If the responses appeared abnormal, the experiment could be repeated to check for malfunctioning equipment or improper electrode position or condition, until a consistent artifact-free response was obtained. This procedure would be greatly facilitated if an on-line computer were available. If the subject was known to have normal vision, the computer would be instructed to recompute the sample mean and variance including the new sample observation, for the twelve parameters of each of the four electrodes and alter its acceptability regions accordingly. This experiment should be repeated for a minimum of 200 people chosen at random from both sexes of the entire population. It should also be incorporated as a standard procedure for all further experiments and each time a normal response is examined, it should be incorporated into the model. Over time, a good approximation to the true population mean and variance should thus be obtained.

The uses of such a model would be manifold. Experimentally, it could be used as a standard of reference. In studying the effect

of different environmental variations on the V.E.P., the results could be described with reference to the model, showing which deflections were affected and by how much. With this fixed frame of reference, published results could be more easily interpreted and repeated. In many publications to date, pathological and experimental results have been compared to so-called normal results based on only one response. Such comparisons are of little meaning, and results thus reported lose some of their significance through the lack of a reliable standard of reference. Also, as pointed out earlier, the beginning of any experiment could be the running of a standard test to determine the normality of the visual system under consideration and to detect the presence of equipment or electrode artifact.

Clinically, the model may someday be a very useful tool. If similar models were defined for the various areas of retinal stimulation, the entire retina could be scanned and tested for normality. This could be used as a supplement or even alternative for the conventional Visual Field Test, which suffers from the disadvantage that its results are influenced by the subject's own judgment in the mapping of the visual field.

It is also conceivable that brain defects and visual system abnormalities could be detected through the use of the V.E.P. parameters by plotting them on the acceptability charts as illustrated in the previous discussion. If a study were performed on several cases of various diseases, it is possible that a particular disease would affect the V.E.P. parameters in a unique way. After considerable experimentation and cataloguing of these pathological cases, the model could someday be used to diagnose the presence of particular diseases, thus reducing the length and amount of preliminary examina-

tion required by a physician.

Summation

Some of the basic analysis and signal processing techniques used in the study of Visual Evoked Potentials have been theoretically outlined or derived, and the underlying assumptions experimentally justified. Certain characteristics of the visual system have been investigated with reference to a simple system model. The nature of the visual response has been examined in detail. A new tool in the form of a statistical model has been proposed for the future study and application of the V.E.P. and an algorithm for the refinement and use of that model has been outlined.

APPENDIX ONE
TECHNICAL SPECIFICATIONS

Stimulator

The stimulus was provided by a Grass model S8C Multifunction Stimulator working in conjunction with a Grass model PS2 Photo stimulator. The full stroboscope flash intensity, when the selector dial was set at intensity four, was approximately 375,000 candle power of duration 10 μ sec.

Shielding

The subject being examined was seated inside an rf shielded room constructed with double steel layered walls, ceiling and floor. The door was similarly constructed with metal leaf around the perimeter to ensure complete shielding and absolute darkness when closed.

Stimulus

A six mm diameter hole was drilled through a removable plate in the shielded room wall. When in position on the wall, the plate made good conducting contact with the wall, maintaining the shielding except for the six mm hole provided for the stimulus delivery. The stroboscope was mounted on the outside of the plate, insulated from it by a cardboard disc, and centered over the stimulus hole. The insulation was used to avoid the possibility of ground loops.

Amplification

Four Grass model P511CR amplifiers were used with voltage gain set at 10,000 and bandwidth 3 Hz-1kHz.

A P.I. eight channel AM-FM recorder was used with speed setting 3.25 inches per second and bandwidth 1kHz on FM.

APPENDIX TWO
THE LOGIC INTERFACE

To enable the transfer of data from the on-line average response computer to the off-line PDP-9 information processing computer, a logic interface was designed and built to read the memory of the on-line computer and transfer it to a paper tape in a format compatible with the PDP-9 reader. Twenty-seven lines were brought out from the "pen" readout circuit⁽¹⁸⁾ of the average response computer into the interface "jam-transfer" register. The ten lines A^0 to A^9 correspond to the address of the data word in the memory and were brought out for possible future use. The lines M^0 to M^{17} constitute the data information itself. These two words were punched onto the paper tape in a five-row format compatible with the PDP-9 tape reader.

The address was punched onto the first five bit locations of the first two rows of the information block. The data information was punched in the binary mode* in the remaining three columns to indicate the information mode to the computer. The first data row contains the sign bit and the four most significant bits, the second row the next most significant bits, and the last row, the least significant bits. The computer was programmed to convert the seventeen bit binary word into an eighteen bit word by shifting the sign bit to the more significant location and substituting the appropriate 1 or 0 in its place. Figure A2-1 illustrates the data and address transfer sequence. Only the data information was read into memory by the PDP-9.

The operation of the interface can be easily explained with reference to Fig. A2-2. Two external timing pulses control the

* Alpha Numeric and Binary are the two alternate modes in which data may be read into the PDP-9 computer. They are outlined in the PDP-9 User's Handbook⁽¹⁹⁾.

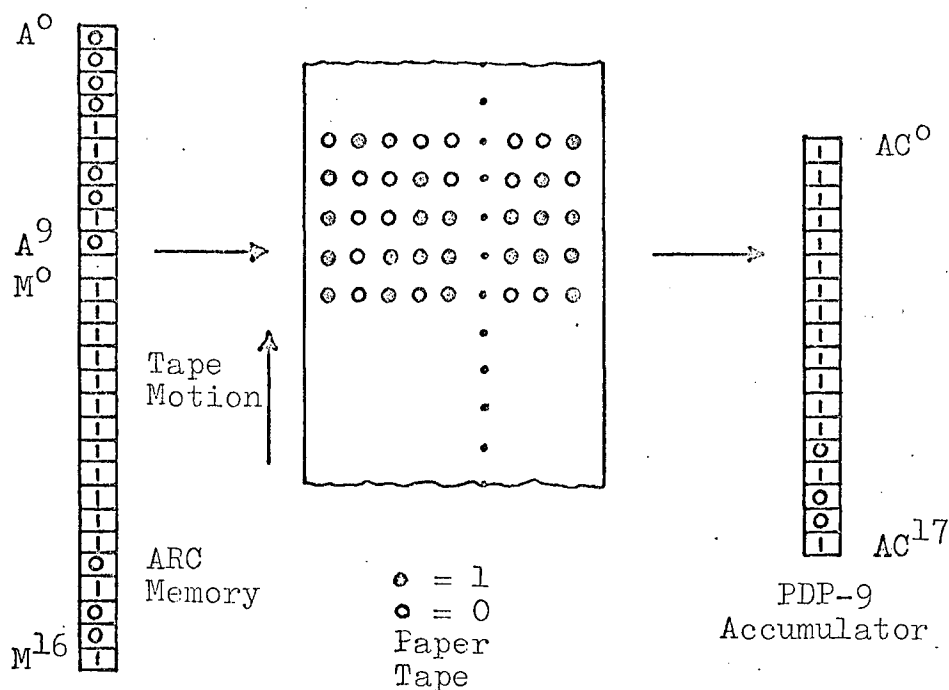


Fig. A2-1 Data Transfer Sequence

sequence of operation events. While the mechanical punch is idling, it continuously sends a timing pulse to the interface each time the punching mechanism passes through the beginning of a punching cycle (maximum of 120 times per second). When the computer "pen" readout button is pressed, the TMV ("Transfer memory to vertical") pulses are sent to the interface at a rate determined by a multivibrator within the "pen" circuit of the average response computer⁽¹⁸⁾. This rate was set at the maximum value permitted by the punch speed. On arrival of the TMV pulse, the readout sequence of the interface is triggered and the punch timing pulse is used to control the scanning of the "jam-transfer" register, in blocks. When readout is complete, the scanning mechanism is automatically disabled until the arrival of the next TMV pulse. The heart of the enable-disable mechanism is a single bit shift register sampling mechanism, the operation of which is discussed in Appendix Three, under "encoding". The average response computer can be set to automatically punch out the entire 1023 words of memory

or any one of the four 255 word quadrants. Since four signals were processed simultaneously, the latter mode was generally used. The interface was hardware programmed to punch out the information onto the tape in the format of Figure A2-1.

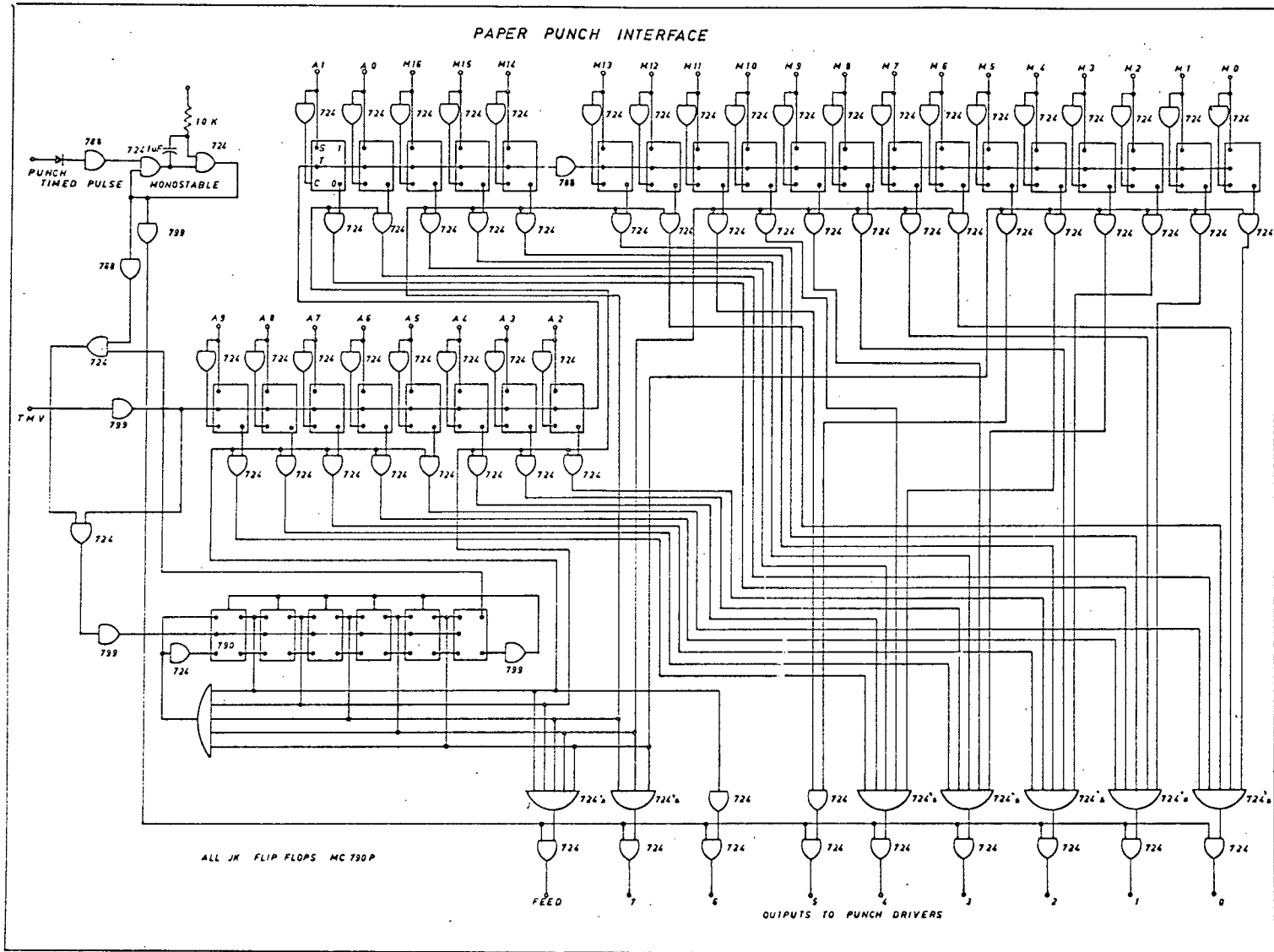


Fig. A2-2 Paper Punch Interface

APPENDIX THREE

DATA CATALOGUING SYSTEM

As was described in the thesis, the analog data obtained during each experiment was stored permanently on magnetic tape for future reference and/or further processing. Since this raw data was frequently re-used and examined, an efficient tagging and cataloguing scheme was deemed desirable. For this purpose, an integrated circuit digital encoder-decoder system was designed and built. Visual monitoring of the coding was also provided and proved of great assistance in the accumulation and processing of the data as well. The system worked on-line in conjunction with the Grass photo stimulator and the eight channel tape recorder.

Encoding

The function of the encoder was to place a unique binary code on the fifth channel of the tape recorder synchronously with the four channels of data, immediately following the delivery of the stimulus to the subject. As well as providing the stimulus flash, the photo stimulator produced a synchronous pulse which was used to trigger the encoding mechanism. On receipt of this pulse, the encoder generates a serial string of 14 positive and negative pulses which are recorded on the tape recorder along with the four visual responses. The first and last bits of the code are always positive or "1" bits and are used as alignment pulses by the decoder as is explained in the decoding section. The center twelve pulses correspond to a binary number with a 1 being represented by a positive pulse and a 0 by a negative pulse. Provision was made for visual monitoring of the code as it was recorded and records were kept of the data location as

desired. The stimulus pulse was also recorded on a sixth channel for use in decoding as will be explained later. A circuit diagram of the encoder is provided in Figure A3-1. The heart of the encoder is a continuously running astable multivibrator which determines the bit rate of the serial output. This rate, 80 Hz, is in turn determined by the frequency response of the tape recorder. At 3.25 inches per second tape speed, the high frequency cut-off of the tape recorder response was 1 kHz. It was found that at this speed, a clock frequency of 80 Hz was the best compromise between speed and pulse distortion produced by the low cut-off of the recorder. The encoder alone however, is capable of operation into the kHz range.

Other main components of the circuit are a binary counter (of 12 bits), a "single bit" shift register (of 15 bits), a logic network, and an output stage. The single bit shift register is gated such that only a single 1 can reside anywhere in the register at any one time. This 1 is shifted to the last register position and is shifted down the register by the clock until it again reaches the last bit location. The output stage has two inputs driven by the two outputs of the logic network in such a way that only one input can be driven at any one time. The purpose of the output stage is to generate a positive or negative pulse depending on which input is pulsed by the logic network.

At the beginning of a tape, the binary counter was reset manually to zero. On the arrival of the first stimulus pulse, the counter is incremented to 1 and the single bit shift register is triggered. As the single bit is shifted down the register, the binary code is read by the logic network a bit at a time, starting at the most significant bit and working down to the least significant, gener-

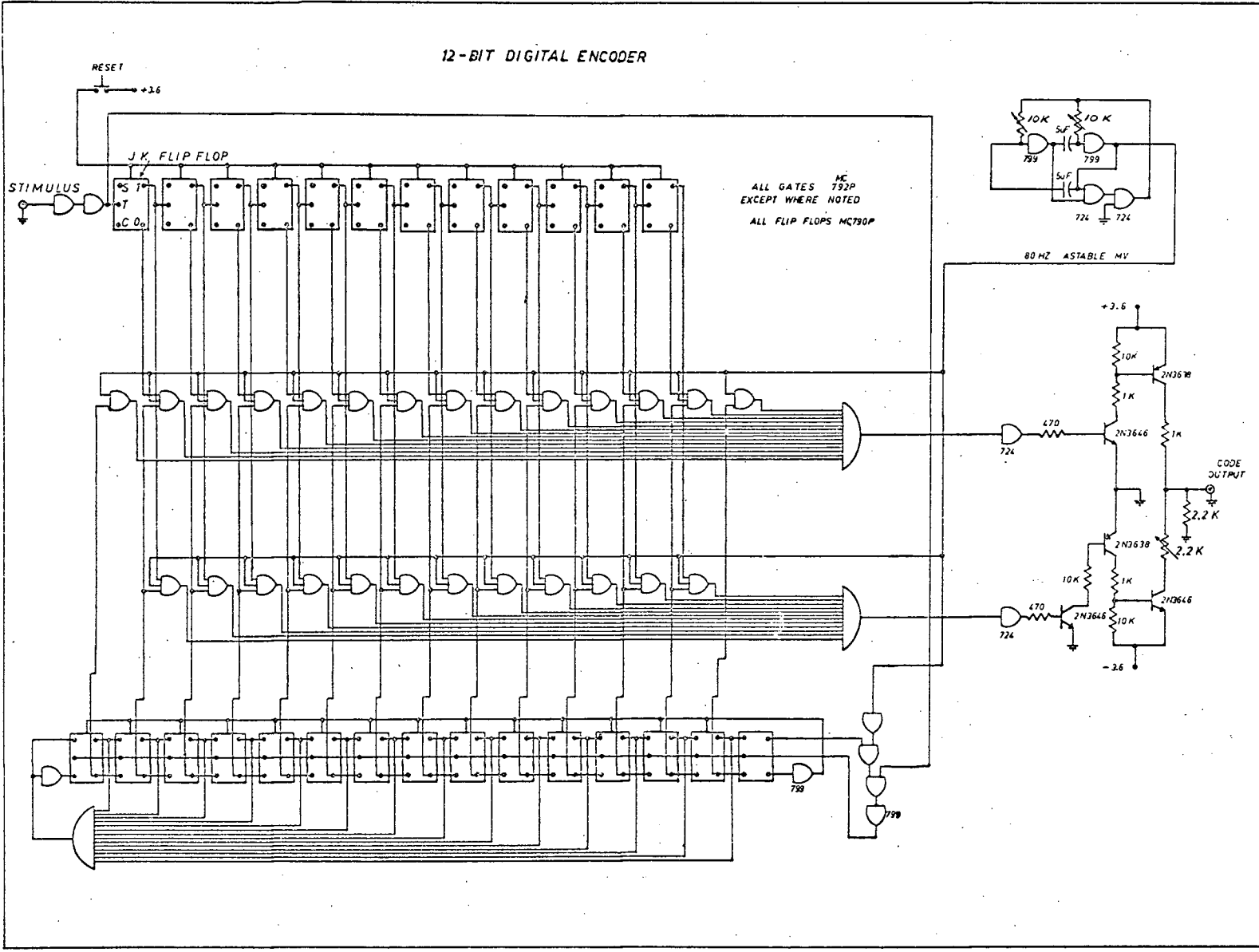


Fig. A3-1 Digital Encoder

ating an output pulse for each bit as it goes. The output pulse is negative if a zero is read and positive if a 1 is read. Visual monitoring of the code was provided through the use of the jam-transfer register in the decoder.

Decoding

The decoding mechanism was used during the playback of data on the tape recorder and to start and stop the averaging of that data on the average response computer. Basically, the stimulus pulse used to start the averaging process and to control its timing, was delivered to the average response computer via the decoder. The decoder controlled the delivery of that pulse in a prescribed manner, hence controlling the data included in any averaging sequence. The decoding circuit diagram is shown in Figure A3-2. The main components consist of: an initial code conditioning and delay network at the input; a shift register; two multiple input nor gates; whose inputs are governed by two sets of switches; and a set-reset flip-flop network controlling the stimulus pulse delivery. To process a given set of data, the first row of switches are set to the address of the response immediately preceding the first response to be included in the averaging process. The second set of switches are set to the address of the last response to be included in the averaging process. The tape recorder is started and the decoder examines each code as it enters the register until the prescribed code is detected. The triggering pulse is then fed to the computer and the averaging process starts. The encoder continues to allow the delivery of the stimulus pulse to the computer until the stop code is detected in the register. The computer is then stopped by the removal of the triggering pulse and

the averaging is completed.

Visual monitoring of each code as it enters the decoder is provided by the jam-transfer register. A switch is also provided to permit continuous reading of the successive codes, or to display only the codes specified by the switches as they are detected.

The input network consists of three branches, a toggle branch, a set branch, and a reset branch. The toggle branch simply converts all input pulses to positive pulses, and applies them to the toggle input of the shift register. The set line receives only the positive pulses, delays them by the switching time of the four 724s, and applies them to the set terminal of the first bit of the shift register. The reset line receives only the negative pulses, converts them to positive pulses, delays them by the switching time of the 724s, and applies them to the reset terminal of the shift register. Because of the inherent noisy output of the tape recorder^{*}, redundancy was built into the system. As was pointed out earlier, two marker pulses were generated at the beginning and end of the code by the encoder. The decoder uses these pulses to determine when the code is completely into the register before detecting and displaying it. A monostable multivibrator was also used to reset the register and its period was made sufficiently long so as to prevent extraneous pulses from entering the system and causing false readings.

* Extraneous pulses were often generated when the tape recorder was stopped or started during the course of an experiment. Also, dirt on the tape sometimes had the same effect.

12 - BIT DIGITAL DECODER

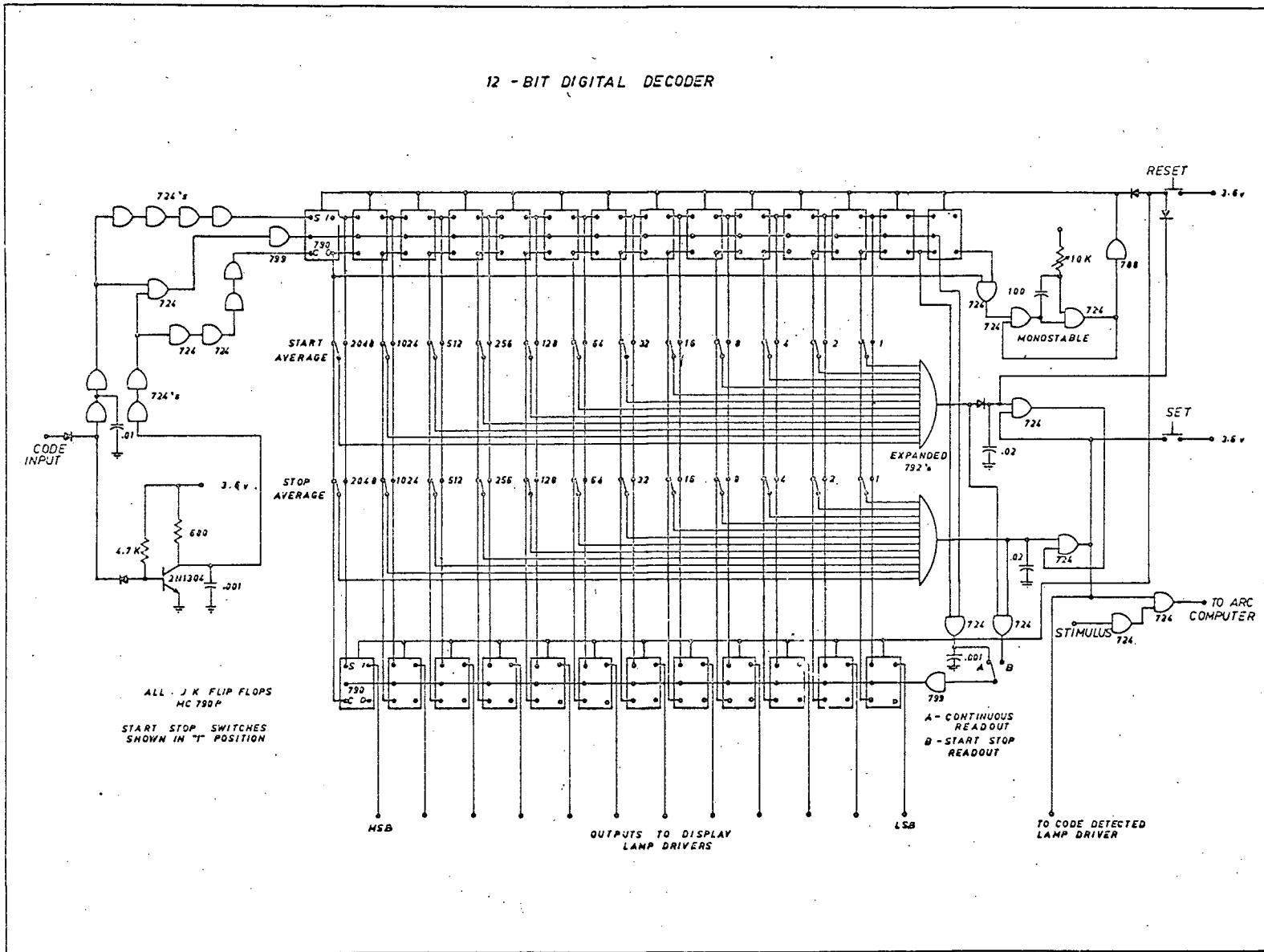


Fig. A3-2 Digital Decoder

REFERENCES

1. Werre, P.F. and Smith, C.J., "Variability of Responses Evoked by Flashes in Man", E.E.G. and Clinical Neurophysiology, Vol. 17:644-652, 1964.
2. Rietveld, W.J., "The Occipitocortical Response to Light Flashes in Man." Acta Physiol. Pharmacol. Neerl., Vol. 12: 373-407, 1963.
3. Ciganék, L. "The E.E.G. Response (Evoked Potential) to Light Stimulus in Man", E.E.G. and Clinical Neurophysiology, Vol. 15: 1961.
4. Creutzfeldt, O.D., and Kuhnt, U., "The Visual Evoked Potential; Physiological Developmental, and Clinical Aspects", E.E.G. and Clinical Neurophysiology, Suppl. 26: 67.
5. Vaughan, H.G., "The Perceptual and Physiologic Significance of Visual Responses Recorded from the Scalp in Man", E.E.G. and Clinical Neurophysiology, 203-223, 1966.
6. Rietveld, W.J., and Tordoir, W.E.M., "The Influence of Flash Intensity Upon the Visual Evoked Response", Acta Physiol. Pharmacol. Neerl. Vol. 13: 160-170, 1965.
7. Wolf, E. "The Anatomy of the Eye and Orbit", Third Edition, 1948.
8. Sances A., and Larson, S.J., "Evoked Potential Recording: An Adjunct to Human Stereotactic Surgery", I.E.E.E. Transactions on Bio-Medical Eng., BME-14:#3, July, 1964.
9. Bendat, J.S., "Interpretation and Application of Statistical Analysis for Random Physiological Phenomena"., I.R.E. Transactions on Bio-Medical Electronics, BME-9: Jan., 1962
10. Bendat, J.S., and Piersol, A.G., "Measurement and Analysis of Random Data", John Wiley and Sons: 1966.
11. Brazier, M.A., "Varieties of Computer Analysis of Electrophysiological Potentials", E.E.G. and Clinical Neurophysiology, Suppl. 26: 1967.
12. Garcia-Austt, E., Bogacz, J., and Vanzulli, A., "Effects of Attention and Inattention upon Visual Evoked Response", E.E.G. and Clinical Neurophysiology, Vol. 17: 136-143, 1964.
13. Gastaut, H., Regis, H., Lyagoubi, S., Mano, T., and Simon, L., "Comparison of the Potentials recorded from the Occipital Temporal and Central Regions of the Human Scalp, Evoked by Visual, Auditory and Somato-Sensory Stimuli", E.E.G. and Clinical Neurophysiology, Suppl. 26:42-52, 1967.

14. Eason, R.G., Oden, D. and White, C.T., "Visually Evoked Cortical Potentials and Reaction Time in Relation to Site of Retinal Stimulation", E.E.G. and Clinical Neurophysiology, Vol. 22: 313-324, 1967.
15. Cazzullo, C.L., Dubini, S., Lucioni, R., Monterisi, G.C., and Pietropolli-Charmet, G., "Evaluation of Photically Evoked Responses in Man by Graphic Superimposition, Automatic Averaging and Selected Frequencies", E.E.G. and Clinical Neurophysiology, Suppl. 26: 42-52, 1967.
16. Rémond, A., and Lesevre, N., "Variations in Average Visual Evoked Potential as a Function of the Alpha Rhythm Phase ("autostimulation")", E.E.G. and Clinical Neurophysiology, Suppl. 26: 42-52, 1967.
17. Barlow, J.S., "Rhythmic Activity Induced by Photic Stimulation in Relation to Intrinsic Alpha Activity of the Brain in Man", E.E.G. and Clinical Neurophysiology, 1960
18. Fabri-tek Instrument Division, "FT-1050 Signal Averager Instruction Manual", 1966.
19. Digital Equipment Corporation, "User's Handbook" (PDP-9).